UNIVERSITÀ DEGLI STUDI DI MILANO

Dipartimento di Veterinaria e Scienze Animali (DIVAS)

PhD Course in Veterinary and Animal Science

Class XXXV

Innovative Imaging of urinary system in canine and feline patients

Candidate: Dr. Carlotta Spediacci

Supervisor: Prof. Mauro di Giancamillo

Co-supervisor: Dr. Maurizio Longo

PhD course coordinator: Prof Fabrizio Ceciliani

2019-2022

INDEX

Abstract

Diseases of the urinary system are regularly encountered in daily veterinary practice. The development of increasingly efficient diagnostic tools is crucial to meet the high-quality requirements of contemporary professional standards.

This project had many purposes, aiming to describe pioneering methods, protocols and diagnosis related to imaging of ureters and urinary bladder, chosen as they represent daily diagnostic challenges in daily routine practice.

This project consisted of three papers: the first paper is a prospective pilot project concerning quantitative CEUS exam applied to distinguish neoplastic and non-neoplastic lesions of the urinary bladder in small animals; the second paper is a multicentric retrospective observational project describing the CT appearance of a novel CVC congenital malformation; the third paper is a retrospective study conducted on canine healthy patients, aimed at assessing the visibility of the ureters on high field MR on T1 and T2 sequences avoiding the use of paramagnetic contrast agents.

The results of this project allowed to obtain objectifiable parameters for the distinction of neoplastic and non-neoplastic lesions of urinary bladder using quantitative CEUS; we also

described the CT appearance of the transcaval ureter, a malfomaration of the CVC never described in veterinary medicine; finally, we described the feasibility of evaluation of normal ureters through high-field MR on T2-weighted sequences, in healthy canine patients.

In conclusion, this project allowed to describe new diseases that could affect urinary tract function and contributes to the development of new methods and protocols with the potential to reduce the invasiveness of certain diagnostic procedures related to the urinary tract.

1. INTRODUCTION AND AIM OF THE STUDY

In recent decades, the need to develop increasingly advanced diagnostic and therapeutic methods in veterinary medicine has grown enormously. Updating and constant research are therefore essential to meet this demand.

The urinary system plays an important role in excretion of the waste products and maintenance of electrolyte balance. Pathologies of the urinary system can be related to metabolic disturbances and derangements of fluid, electrolyte and acid-base balance.[1]

Diseases of the urinary system are part of the daily routine in veterinary medicine practice.

When assessing a patient with lower urinary tract disease, signalment can be very helpful in formulating the list of possible aetiologies. For example, younger cats are more likely to have

idiopathic disease than older cats.[2] Sex is also important in pointing towards a diagnosis, as females are predisposed to lower urinary tract infections. [3] Knowledge of the predisposition of breeds to specific lower urinary tract diseases will also help focus diagnostic efforts. For example, Bichons are predisposed to developing calcium oxalate stones, male Dalmatians are predisposed to developing urate stones and older Scottish Terriers have a predisposition to urothelial cell carcinoma (UCC).[4;5]

A complete and detailed medical history from the owner is the first essential step. Specific questions should cover the patient's general attitude and activity level, water consumption, frequency and pattern of urination, abnormalities in the smell or color of urine. In addition, information on all previous treatments and response to therapy should be obtained. Disease of the lower urinary tract have characteristic clinical

signs that are usually, but not always, present. Most of the times multiple clinical signs are present and indicate the necessity of further evaluation oriented on the urinary system. These clinical signs include dysuria, stranguria, pollakiuria, periuria and urethral obstruction and hematuria (MacLeod et al, 2011).

Once these symptoms have been identified, it is necessary to include a wide range of possible causes of the problem in the differential diagnoses, which include degenerative, congenital, metabolic, neoplastic, behavioral, inflammatory, infectious, idiopathic, ioatrogenic, traumatic and toxic ethiologies. hematuria (MacLeod et al, 2011).

A thorough physical examination is the second key step to a correct diagnosis, including abdominal palpation, transrectal palpation with evaluation of urethra, urethral tone and possible prostathetic disease. A palpation of the abdomen can be used to assess the size and turgor of the bladder. Palpation of the

abdomen may also be useful to identify pain. Transrectal palpation of the urethra may be used to identify urethroliths, urethral tumours, urethral tone and prostatic disease, all of which may contribute to lower urinary tract signs.[6]

Considering this information, it is intuitive that imaging is essential to reach a specific diagnosis of diseases of the urinary system in order to establish a correct treatment.

The diagnostic methods for evaluating the urinary tract include radiography (intravenous excretory or retrograde cystography or urethrography), ultrasonography, computed tomography, magnetic resonance imaging, and renal scintigraphy for functional studies.

Of these techniques, the most readily available are undoubtedly radiography and ultrasound, while the remaining methods are more expensive and less readily available in veterinary medicine.

This project has multiple objectives, which aim to describe pioneering methods, protocols and diagnoses related to the imaging of the urinary system in dogs and cats.

The first aim is to describe the sensitivity and specificity of quantitative CEUS in the diagnosis and distinction between neoplastic and non-neoplastic diseases of the urinary bladder in canine patients.

The second aim describes in detail the tomographic aspects and clinical signs of a novel congenital pathology, the transcaval ureter. This anomaly is described as rare in humans and has never been previously described in veterinary medicine.

Finally, we described the appearance, course and characteristics of the ureters from the renal pelvis to the ureterovesical junction using a high-field MRI in multiple sequences, without using a gadolinium contrast agent, assessing also whether and which factors may influence good image quality in order to optimize patient preparation and the diagnostic MRI protocol. This novel

diagnostic MR protocol would be particularly suitable in patients where renal excretory function is significantly reduced, and intravenous contrast medium is therefore contraindicated.

2. DIAGNOSTIC IMAGING OF URINARY SYSTEM: STATE OF ART

2.1. Radiography

2.1.1. Indication and procedure

The radiographic technique is used to assess changes in the size, shape, symmetry, opacity and number of kidneys, retroperitoneal space, urinary bladder and urethra. The indication for a radiographic examination includes histories of trauma, suspicion of masses, urinary obstructions secondary to stones and/or masses.[7]

For a complete evaluation of the abdomen, the three projections, left and right lateral and ventrodorsal, are obviously necessary; Moreover, the three-standard projection of the abdomen are an essential step before any contrastographic study. [8]

2.1.2. Radiographic appearance of urinary system

Dog kidneys are oval-shaped and located in the retroperitoneal space and are surrounded by an adipose layer. The cranial pole

of the right kidney is usually barely visible because it overlaps the caudate lobe of the liver. The right kidney is located at the level of the 13th rib while the left is slightly more caudal, between L1 and L3. In addition, the left kidney being more mobile may locate more ventrally than the right.[9]

Cat kidneys also have an oval shape and are located between L1 and L4, more or less at the same level or with the right one being slightly more cranial.

The maximum size of the kidney has been described in relation to the second lumbar vertebra. In dogs, the kidneys normally measure 2.5 to 3.5 times the length of L2. In cats they usually measure between 2.4 and 3.0 times the length of L2. [10]

In cats a hormonal influence on kidney size has also been demonstrated, with both males and females having larger kidneys.[11]

Normal kidneys have uniform tissue radiopacity, although fatty deposits may cause focal radiolucency centrally. In contrast,

mineralization is always abnormal but not necessarily responsible for clinical signs.

The urinary bladder is located in the caudo-ventral abdomen and may be displaced abnormally in different directions. [12;13]

In the case of severe displacement of the urinary bladder, as in the case of a hernia, the urinary bladder may not even be discernible radiographically and cystography or ultrasound may be necessary for its identification. Retroflexion of the urinary bladder has been observed in 24% (10/41) of dogs with perineal hernia.[14] A urinary bladder partially within the pelvic canal may be associated with congenital abnormalities of the urinary tract. A pelvic urinary bladder has been reported to be a normal variation.[15]

Female incontinent dogs with a pelvic urinary bladder usually have a significantly shorter urethra than continent dogs.[16;17]

Since pelvic urinary bladder does not always suggest a clinical problem, pelvic urinary bladder must be correlated with clinical signs to determine its significance.

With conventional radiology there are few visible changes to the urinary bladder. What can be assessed is the state of repletion, size, and opacity for example to assess the presence of radiopaque stones.

Insufficient radiographic visualization of the urinary bladder is likely to occur regardless of abdominal contrast. If the serosal contrast is good and the urinary bladder is not visible, the urinary bladder is empty or has been displaced caudally or ventrally. If the serosal contrast is bad and the area of the urinary bladder is not clearly visible, the cause may be free peritoneal fluid or inadequate peritoneal fat.

A shape modification of the urinary bladder is uncommonly visible. Abdominal masses adjacent to the serous surface of the urinary bladder may distort its shape. Tumors that arise from the

wall of the urinary bladder occasionally bulge from the serosal surface and cause a discernible change in the shape of the urinary bladder, but it is uncommon.[18]

Any radiographic change of the opacity within the urinary bladder is abnormal and usually easily detected. Gas in the urinary bladder may be introduced iatrogenically by catheterization or cystocentesis. Gas in the lumen of the urinary bladder, into the urinary bladder wall and occasionally into the ligaments of the urinary bladder is present in emphysematous cystitis. Emphysematous cystitis is produced by glucose-fermenting organisms and may be seen in association with diabetes mellitus.[19;20] Emphyshaematous cystitis without diabetes mellitus may also be found.

The majority of increased opacities associated with the urinary bladder are calculi. It is also possible to confirm the presence of stones by a compressive view to move adjacent structures that overlap or surround the urinary bladder or by ultrasound. If

cystic stones are identified, it is necessary to examine the rest of the urinary tract from the kidneys to the end of the urethra for the presence of other stones. Since not all stones are radiopaque, the absence of radiopacity within the urinary bladder does not exclude the presence of cystic stones.

2.1.3. Congrastographic radiography

Excretory urography

Nonionic organic iodides are given intravenously as a bolus and are excreted by the kidneys by glomerular filtration followed by tubular water reabsorption.

Too often, probing radiographs provide insufficient information regarding disorders of the upper urinary tract. Because of these inherent limitations of plain radiographs, excretory urography has proven to be a valuable tool to further evaluate both the kidneys and ureters.

The examination is a relatively simple means of verifying and localizing diseases of the upper urinary tract. Although

excretory urography is not a quantitative measure of kidney function, it can be used to assess the relative function of the kidneys. In addition, the information obtained can sometimes provide information that can be used to assess the pathophysiological mechanisms of renal failure. For example, acute tubular necrosis will be associated with different opacity changes than chronic glomerular disease.

The excretory urogram consists of a nephrogram phase and a pyelogram phase. In the nephrogram phase, contrast medium entry into the glomerular vessels and filtration into the nephron leads to uniform opacification of the renal parenchyma. At first, the cortex may be opaquer than the medulla. The nephrogram starts after about 10 seconds and persists for up to 2 minutes, till the pyelogram phase begins and the nephrogram begins to fade. In the pyelogram phase, the opacity of the nephrogram should continue to decrease. The contrast medium is concentrated in the renal tubules as a result of water reabsorption and is excreted

into the renal pelvis with its diverticulae and into the ureters. If renal function is normal, the collector system is always opaquer than the renal parenchyma. The normal renal pelvis is curvilinear and less than 2 mm wide.[21]

Three factors - glomerular filtration, renal concentration capacity and hydration status of the patient - influence the quality of the study. The contrast medium is passively filtered by the glomerular filtration, and any reduction in filtration decreases the amount of excreted radiopaque material and thus the density of the renal image. Renal concentrating capacity is critical because reabsorption of water in the tubules increases the density of contrast within the kidney and ureter. Since the renal tubules are unable to reabsorb the contrast medium, the amount of water that can be reabsorbed produces a higher concentration of the contrast medium. This higher density/concentration results in better visualization of the collector system. Finally, adequate hydration of the patient is essential to ensure proper

renal perfusion, and thus globular filtration and renal concentration capacity.[23-25]

Impaired kidney function may result in increased excretion by alternate routes through the liver into bile and into small intestine. The use of excretory urography has decreased due to the wide availability of ultrasound and advanced imaging. Suspected trauma to the kidney or ureters, haematuria, ectopic ureter and suspected retroperitoneal mass are indications for this technique.

Intravenous contrast medium iodine-induced adverse reactions, such as nausea, vomiting, urticaria, hypotension and contrast medium-induced renal failure, are infrequent but occur occasionally. Using non-ionic contrast media leads to fewer complications due to lower osmolarity. The risk factors for contrast medium-induced nephropathy include renal insufficiency and poor hydration status. Contraindications for

excretory urography, then, include anuric renal insufficiency, dehydration or hypotension and known hypersensitivity to iodinated contrast media.[26;27]

Anterograde Ultrasound-Guided Pyelography

The ultrasound-guided injection of contrast medium into the renal pelvis leads to outstanding opacification of the collector system because the contrast medium is not diluted and its occurrence in the collector system is not dependent on renal function. This procedure can be carried out in azotemic patients without loss of image quality. In addition, each kidney pelvis and ureter can be assessed individually.

The renal pelvis distends with a mild attenuation of the pelvic diverticula, while the contrast medium is injected with gentle pressure. If the ureter is pervious, the contrast medium should appear almost instantly in the urinary bladder. A narrowing of the ureter due to peristalsis may be observed; repeat imaging will be necessary to distinguish between peristalsis and stenosis.[28]

Anterograde pyelography has been used in the diagnosis and localization of ureteral obstruction and ureteral rupture in dogs and cats.[28-30]

Further advantages are the absence of systemic reactions to the contrast medium and the collection of urine straight from the renal pelvis for urinalysis and microbiological examinations. The main indication for this procedure is suspicion of ureteral obstruction. Contraindications include coagulopathies, because bleeding can occur.

Potential adverse effects include hemorrhage, focal renal tissue damage and spreading infection in the presence of pyelonephritis or pyonephrosis with perirenal sepsis and abscess. Contrast medium may also leak into the retroperitoneal space. The loss of renal function secondary to the procedure is minimal but must be considered in patients with already severely impaired renal function.

Cystography

Retrograde cystography with contrast is a quick, simple and inexpensive technique that can provide valuable diagnostic and prognostic information. Clinical indications for cystography include dysuria, pollakiuria and chronic intermittent or persistent haematuria.

X-ray signs suggestive of the need for cystography include identification of an increased or decreased opacity in the urinary bladder, evaluation of caudal abdominal masses that may be associated with the urinary bladder, non-visualization of the urinary bladder after abdominal trauma, and an abnormal shape or position of the urinary bladder.[31]

Cystography can be performed with positive contrast medium, soluble iodine contrast medium, or negative contrast medium, for which gas is used. The double-contrast technique, which is useful for the evaluation of the bladder wall, is also widely used.

Radiographic signs that can be observed during cystography include irregular mucosal margins, intramural thickening, filling defects and leakage. What can be complex is the distinction between what is pathological and what is artefactual.[18]

Complications from catheterization rarely occur and are usually not life-threatening. Iatrogenic trauma, bacterial contamination or kinked and knotted urethral catheters may be caused by improper catheterisation. Mucosal ulceration, inflammation and granulomatous reactions may occur, but the changes are usually transient and do not produce serious clinical problems. The most serious complication of contrast-negative cystography is gas embolisation in the circulatory system, which can cause death but is very rare.[32;33]

2.2. Ultrasonography

Sonography has become an essential imaging modality in the field of veterinary medicine and is increasing in popularity year by year.

Since the 1960s, sonography has been clinically indicated in animals for many of the same reasons as in humans. Sonography is fast, non-invasive and can greatly improve veterinarians' diagnostic and therapeutic capabilities.

2.2.1. Indication and procedure

Veterinary sonography is used in many different cases. In recent decades, the use of ultrasound for the evaluation of the upper and lower urinary tract has become widespread. The low cost and ease of use have made this imaging technique the first choice in approaching patients with symptoms referable to the urinary tract.

The most common indications for performing an ultrasound examination of the urinary tract are:

- haematuria,
- pyuria,
- proteinuria,
- suspected urolithiasis,
- acute renal failure,
- chronic renal failure,
- polyuria and polydipsia,
- reduced abdominal detail on radiography,
- congenital renal dysplasia or familial nephropathies.

Suspicion of urinary tract pathology is therefore sufficient reason to perform an ultrasound examination.[33]

Ultrasound makes it possible to diagnose numerous disorders of the urinary system. Through the evaluation of profiles, dimensions, vascularization and organ echogenicity, congenital kidney and ureteral pathologies, acute and chronic infectious/inflammatory pathologies and neoplastic pathologies can be detected. Ultrasonography is also used for diagnosis of

ureteral obstruction, that can be challenging. However, accuracy of survey radiography or ultrasonography for detection of ureteral calculi, is only moderate with instances of false-negative and false-positive results having been recorded for both modalities.[7]

Ultrasound is also used to diagnose cystitis (bacterial, pseudomembranous, emphysematous, polypoid), inversion of the urinary wall, congenital malformations (septa, bladder duplication), neoplasia (Urothelial cell caricinoma most common).

Before the ultrasound examination, the animal's hair must be cut, and an ultrasound gel applied to its skin to optimize images of the kidneys and other organs. Patients may be scanned in dorsal, left or right position.

In order to perform ultrasound examination of the kidneys, the transducer with the highest frequency that allows adequate

penetration must be used. In small dogs and cats, 7.5 to 15 MHz transducers are appropriate; 5 MHz or lower frequency transducers should only be used in large dogs. Subcostal or intercostal windows with the patient in sternal or dorsal recline allow access to the kidneys, depending on patient size and thoracic conformation. Images should be acquired in dorsal, sagittal and transverse planes, always followed by fanning the transducer across the entire kidney. The renal pelvis is best seen in the dorsal and transverse planes. The ureters may be followed caudally by the renal pelvis if dilated. To verify the patency and normal position of the ureterovesical junction, the bladder must be assessed for the presence of two jets of urine from the dorsolateral bladder wall.

In some animals it is necessary to administer a diuretic to increase the frequency and visibility of ureteral jets in the bladder.[34]

The urinary bladder must be assessed in a transverse plane and

orthogonally in a sagittal or dorsal plane. An accurate assessment of the thickness of the urinary bladder wall requires a perpendicular alignment of the ultrasound beam to the urinary bladder wall.[34]

2.2.2. Ultrasonographic appearance of urinary system

The kidneys may be oval, particularly in cats, or bean-shaped, more commonly in dogs.[35;36] Kidneys have to be measured in all planes and volumes can be estimated.[7] Renal size and degree of pelvic dilation are variable in cats with normal renal function, and normal values overlap with values observed in cats with renal disease or urinary obstruction.[37;38] Renal length in normal cats usually varies between 3.0 and 4.5 cm and is influenced by breed. The kidneys are also typically larger in intact cats and often become smaller with advancing age. The right kidney may also be longer than the left.[39]

Renal length can also be compared with the diameter of the aorta or the length of L5 or L6 in dogs.[35;36]

The renal medulla is hypoechogenic with respect to the cortex, which is usually hypo- or isoechogenic with respect to the liver and typically hypoechogenic with respect to the spleen. In cats, the accumulation of fatty vacuoles in the renal cortex appears to contribute to its hypereogenicity.[40] The medulla appears separated into several lobulated segments by the presence of linear echogenicities representing the boundaries of interlobar vessels and diverticulae. The medulla, parallel to the cortex below the arcuate arteries, may also be isoechoic to the cortex, giving the impression of cortical thickening, or even hyperechoic to it, forming a hyperechoic band superficial to the arcuate arteries. The renal crest is the extension of the renal medulla and is in contact with the pelvis.

The walls of the arcuate arteries can be observed as short, paired

hyperechoic lines at the corticomedullary junction. These vessels, as well as the larger renal and intralobar vessels, can also be assessed with colour Doppler or power Doppler. Pelvic height in dogs and cats usually measures less than 2 mm when using a transverse plane, although it can sometimes exceed 3 mm.[41] One study found that a renal pelvic diameter > 13 mm was consistently associated with ureteral obstruction, but the majority of obstructed kidneys have less marked pelvic dilatation, so may appear similar to kidneys affected by chronic renal failure or pyelonephritis, which also frequently exhibit pelvic dilatation.[38]

In contrast, ureters are not normally visible in dogs and cats. The pelvis is surrounded by the sinus, which contains fat and appears hyperechoic and is particularly prominent in obese cats.

Ultrasound examination of the urinary bladder is rapid, does not expose the patient or operator to ionising radiation, does not require urinary catheterisation and rarely requires a sedation.[42]

Ultrasound allows direct visualisation of mucosal and serosal margins, and bladder wall thickness can be measured directly from static images.

Ultrasound allows the identification of structural pathologies of the bladder wall.[43]

The urinary bladder is located in the caudoventral abdomen and the urethra extends into the pelvic canal. The descending colon, aorta and caudal vena cava are dorsally located to the urinary bladder.

Air within the colon, combined with the curved interface of the bladder wall, can cause artefact of the urinary bladder.

The four histological layers of the bladder wall are the mucosa (hypoechoic), the submucosa (hyperechoic), the musculature (hypoechoic) and the serosa (hyperechoic). However, these

layers are difficult to define by ultrasound. The thickness of the bladder wall decreases as the volume of the urinary bladder increases. Normal bladder wall thickness in cats has been reported to be up to 1.7 mm.[44]

Furthermore, normal bladder wall thickness increases up to 1 mm with increasing body weight in dogs.[45] The trigone of the bladder is not clearly delineated from the rest of the bladder wall. The entrances of the ureter into the urinary bladder are not usually visible, except if there is dilatation. Ureteral papillae may be seen extending from the mucosal surface of the dorsal wall and should not be confused with other causes of focal thickening of the wall. Urine jets may be observed emerging from the dorsal bladder wall at the trigone. These ureteral jets appear as an eruption of hyperechoic speckles on B-mode ultrasound or as a positive signal pulse on color flow Doppler. Imaging of ureteral jets is variable because it requires a difference in specific gravity

between urine in the bladder and urine exiting the ureter. To improve visualization of ureteral jets within the urinary bladder, intravenous furosemide (1 mg/kg) can be used.[46] Normal urine inside the urinary bladder is almost always anechoic.[34]

A common pathological finding is an outgrowth in the bladder secondary to a transitional cell carcinoma. These masses tend to be located in the trigone of the urinary bladder and can often be clinically related to a dog/cat's effort to urinate.

The urethra elongates caudally from the bladder into the pelvic canal.[34]

In male dogs, the prostate surrounds the proximal urethra. The shadow of the pubis obscures the caudal intrapelvic portion of the urethra. The proximal penile urethra is placed within the spongiosus body between the corpus cavernosum dorsally and the bulbospongiosus and retractor muscles of the penis ventrally. The distal penile urethra is

situated within the urethral groove of the os penis dorsally and the bulbus glandis ventrally. The urethral lumen is not normally visible unless there is distention of the urinary bladder, in which case urethral obstruction must be considered. The urethral wall is formed by the histologic layers of the urinary bladder. These layers are not easily visible when they are normal.[34]

2.2.3. Contrast-enhanced Ultrasound

Contrast-enhanced ultrasound (CEUS) consist of gaseous microbubbles wrapped in an adipose envelope.

2.2.3.1. *Technique and procedure*

The most popular contrast media are Definity (Lantheus Medical Imaging, North Billerica, MA), Sonovue (Bracco Imaging, Monroe Township, NJ) and Sonozoid (Daiichi-Sankyo, Tokyo, Japan). Each of them has specific indications for preparation, administration, and storage.
As mentioned above, these contrast media consist of 'bubbles'

with two components: an inert fluorocarbon gas wrapped in a lipoprotein layer.[47]

Sedation is not usually necessary but reducing the patient's movement can be helpful. The patient must be prepared for a standard ultrasound, so a trichotomy is necessary.

Once the patient and contrast medium have been prepared, the organ or lesion of interest is identified with greyscale ultrasound. The ultrasound system settings are then modified for CEUS imaging. Prior to contrast medium injection, the image is essentially signal-free, as the greyscale image is subtracted. Most systems allow a dual screen where the greyscale image is presented simultaneously for anatomical reference.

The contrast medium is bolus injected, followed by a saline flush. If available on the ultrasound system, a counter can be initiated at the time of injection for future reference on contrast medium inflow times and peak enhancement.

The dosages are quite small, depending on the medium used, and range from 0.1 to 1.0 mL. Therefore, all contrast administrations must be immediately followed by sterile saline to push the contrast into the port or catheter towards the patient. Microbubbles are easily distortable and destructible.[48] Distortability allows the compression and rarefaction of incident waves to reduce or increase the diameter of the bubbles. With very low incident sound energy, the bubbles change size linearly, increasing and decreasing in a sinusoidal pattern directly proportional to the ambient pressure. However, at higher incident sound energy, the bubbles act non-linearly, spending more time expanding than compressing. A frequency analysis of the signal transmitted by the bubbles at this energy level reveals the frequency of the incident sound and additional sound signals. With an incident sound of even higher energy, the bubbles are destroyed ('burst'), thus liberating a large amount of incident and harmonic frequency sound energies.[47]

Ultrasound contrast agents, unlike iodine and gadolinium, are strictly vascular agents, without any interstitial component. The contrast effects are the appearance of these bubbles on a black screen, which typically indicate large and small vessels.

2.2.3.2. Clinical application on urinary system

Although CEUS has found wide application in the evaluation of organs such as the spleen, liver and pancreas, it is still very limited in the urological system.

The normal renal vasculature consists of a single large afferent artery that branches into interlobar arteries radiating from the renal hilum through the medulla to the level of the corticomedullary junction. The arcuate arteries radiate perpendicular to the interlobar arteries, parallel to and at the level of the corticomedullary junction. These ramify into interlobular arteries, parallel to the interlobar arteries, which extend to the glomeruli within the cortex. The efferent vessels from the glomeruli supply the proximal and distal convoluted

tubules and loops of Henle. The perfusion pattern in a normal kidney is therefore biphasic and symmetrical, with the cortex perfusing before the medulla.[49]

Various renal lesions, such as nephritis, neoplasia or infarction can cause regional hypoperfusion. This non-specificity precludes accurate characterization but may provide a useful mechanism to better define lesion margins.[49]

2.3. Computed Tomography

Computed tomography (CT) is frequently used for the evaluation of urinary tract. Computed tomography has the advantage of being able to characterize the entire urinary tract without overlapping other structures.

The kidneys, ureters, bladder and urethra can be easily evaluated in CT and their shape, size, location and density and position can be evaluated.

2.3.1. Indication and procedure

Computed tomography (CT) is frequently used for the evaluation of the urinary tract. The indications are essentially the same as for the excretory urogram, but CT has the advantage of being able to visualize the entire urinary tract without overlapping other structures. CT angiography is used for the evaluation of the renal vasculature. It allows evaluation of normal anatomy, anatomical variations and abnormalities. Multiplanar and three-dimensional (3D) reconstructions add valuable information.[50]

Imaging protocols always include a precontrast phase to visualize any mineralization in the renal parenchyma or collector system. In most patients, intravenous contrast medium (400 to 800 mg I/kg body weight) must be administered to delineate renal parenchymal lesions and filling defects in the collector system.[51]

With contrast enhanced CT, the renal parenchyma is enhanced immediately after contrast medium administration.

It was shown that the best opacification of the ureters was achieved with a contrast medium dosage of 400-800 mgl/kg three minutes after injection. With lower dosages on the other hand (100-200 mal/kg), opacification of the ureters was not sufficient. For the evaluation of the ureters and ureterovescical junction repeated scans should be performed on that section of interest.[51]

A prospective study described also the bolus tracking technique as appliable to assess the uretero-vescical junction in healthy patients by placing the region of interest at the level of the distal ureter. This technique reduces also patient exposure to ionising radiation.[52]

Contrast enhanced computed tomography also makes it possible to calculate the glomerular filtration rate and thus renal function.[53]

The measurement of renal function is crucial in the diagnosis and management of kidney disease. The usefulness of any kidney function test is based on sensitivity, specificity and convenience.[54;55] Screening tests, such as blood urea nitrogen (BUN) and plasma creatinine concentrations, are readily available, but these measurements are relatively insensitive.[56] Abnormal BUN and creatinine values are not reached until 67-75% of the nephrons are non-functional.[57;58] Determination of the glomerular filtration rate (GFR) is the most important component in the assessment of renal function in humans and animals with suspected kidney disease. GFR cannot be measured directly. Therefore, it must be estimated by measuring the clearance of a filtration marker.

For many years, scintigraphy was considered the cornerstone of functional imaging.

Since the 1980s, CT has been used to estimate organ function. The first dynamic or functional CT studies concerned the

measurement of cerebral perfusion, later renal, hepatic and cardiac function. The first use of dynamic CT in people to assess kidney function dates back to 1991.

It was not until 1993 that a technique involving Patlak analysis was proposed, using a single position scanning protocol at 5 s intervals for 2 minutes.[59] The use of this method provided a new estimate of GFR, the blood clearance per unit volume (ml/min/ml).[59-61]

A linear relationship exists between changes in attenuation from baseline and iodine concentration, so it is possible to create a relative curve of plasma concentration versus time.[60] From these curves, the contrast clearance per unit volume of an organ, such as kidney, liver or brain, can be calculated using Patlak's graphical analysis.[59;62]

The advantages of functional CT, apart from the determination of GFR for each individual kidney, are that it does not require blood or urine samples, it is quick and easy to perform and the

morphological features of the kidneys can be determined at the same time.

A new technique has also been described that could provide new opportunities for diagnosing symptoms related to the urinary system and for assessing post-surgical adaptation. Using low-dose radiation, the sharply defined image obtained with 4D-CT urodynamic examination can be used as a physiological diagnostic tool to evaluate a series of urinary movements from any angle between prostate, urethra and bladder in a unified manner with the addition of the temporal axis.[63]

Finally, CT angiography is used to assess the anatomy of the renal vasculature, with advantages for surgical planning.[64] Normally, each kidney is supplied by one artery and one vein. However, anatomical variations of additional arteries and veins often occur in the pets.[65] Software applications of CT can be used to quantify renal volume with good accuracy.[65]

Computed tomography (CT) is useful to diagnose abnormalities of the urinary bladder wall and the ureterovesical junction.[51] Computed tomography-excretive urography can be utilized to diagnose ureteral ectopia by tracing the course of the ureters as they enter or continue beyond the ureterovesical junction. The differentiation of extramural and intramural ureteral ectopia has been documented using CT-excretive urography.[51] Advanced imaging of urinary bladder neoplasia in dogs and cats is not widely practiced due to cost and less availability than ultrasound. Both modalities are excellent for the evaluation of the primary lesion, ureters, adjacent lymph nodes and other organs.[6] Neoplasia and lesion of the urinary bladder can be evaluated with CT to determine the extent of the tumor for pre-treatment staging and to evaluate the tumor's response to treatment by volumetric comparison measures.

2.3.2. CT appearance of the urinary system

The distribution and progression of contrast medium is considered crucial in the evaluation of CT studies performed for urinary system disorders.

In normal conditions, the kidneys show tissue density with a thin peripheral halo of adipose density, with homogeneous contrast. The normal ratio of renal length to vertebral body L2 in CT imaging was determined to be 2.7 (95% CI, 2.5 to 2.9) and the ratio of renal length to aorta 7.4 (95% CI, 7.07 to 7.74).[66]

Renal contrast enhancement is multiphasic, as the contrast medium is filtered by the urinary system. The cortex contrast increases to a greater degree than the medullary in the early corticomedullary phase. The nephrogram phase displays uniform renal enhancement before urine collection in the renal pelvis. The renal pelvis and medullary are enhanced during the excretory phase. The ureters fill segmentally with contrast medium as a consequence of peristaltic contractions during the

excretory phase. The ureters insert into the dorsal wall of the bladder near the trigone. The distal ureters are closely connected to the descending colon. A colon full of faeces can make identification of the ureters more difficult. The ureterovesical junction can be seen in normal dogs as small convex structures on the dorsal side of the urinary bladder.[67] Detection of a ureteral jet in the urinary bladder confirms the presence of a normal ureterovesical junction.

The urethra is less commonly assessed with transverse imaging but is easily included in the scan through the pelvis and CT urethrography can be performed to better delineate the urethral lumen.[51]

Images of the parenchymal phase are useful to visualize the mucosa of the ureters, urinary bladder and urethra, which is enriched with contrast.

Images of the excretory phase shall be performed with the pelvis elevated, so that the gravity-dependent contrast-enriched urine

collects in the cranioventral bladder, away from the trigone area and the clinically relevant vesicourethral junction.

The female urethra can be delineated with a retrograde vaginogram study; however, urethral filling is not consistently obtained with this technique.[6]

2.3.3. Adverse reaction

Contrast-induced nephropathy (CIN) has been reported in humans, which causes acute renal damage with a creatinine increase of more than 0.5 mg/dl or 25% over baseline within 48 hours after contrast administration.[68] This phenomenon has not been completely characterized in dogs and cats. The use of iso- and low-osmolar contrast media reduces the risk of CIN, as does pre- and post-contrast hydration with intravenous saline.[68]

A reduced dose of contrast medium (400 mg I/kg body weight) allows adequate image quality, which could be advantageous in patients with impaired renal function.[50;51]

As with excretory urography, limitations include the need for anaesthesia or sedation and the need to administer contrast medium intravenously.[50]

2.4. Magnetic Resonance

2.4.1. Indication and procedure

To date, abdominal MRI has had limited use in veterinary medicine.[69] This is due to the relatively high cost and less availability of MRI, the need for prolonged anaesthesia, advances and increased use of ultrasound and abdominal CT, and technical obstacles such as the effect of respiratory and visceral motion on image quality.

Thanks to the introduction of respiratory gating and the optimal soft tissue contrast resolution the employment of MRI has increased, and it has been used to characterize kidney and collecting system disorders.[70]

However, for the moment CT continue to be the imaging modality of choice for abdominal imaging over MRI for most clinical conditions.

In human medicine, digital subtraction angiography, contrast-enhanced computed tomography angiography and magnetic resonance angiography (MRA) allow for excellent renal vascular imaging.[70] In some institutions, MRA has replaced ultrasound, digital subtraction angiography and contrast-enhanced computed tomography angiography in the evaluation of various renal vascular pathologies, and in the pre- and post-operative evaluation of renal vessels.[70-72] Although ultrasound is still often used as a screening tool for renal artery stenosis, MRA is more accurate, three-dimensional, less operator-dependent, has a larger field of view (FOV) and higher contrast resolution.

Magnetic resonance imaging consists of a machine that generates a stable magnetic field within which the patient is

placed. Hydrogen atoms within the anatomical area of interest being analyzed are aligned to this stable magnetic field. The application of a series of radio frequency (RF) wave pulses with predefined frequencies causes the proton alignment to be temporarily interrupted.

When the protons realign, they generate characteristic RF signals that are detected by the coil and generate the image. The intensity and character of the returning RF signals depend on strictly tissue-specific characteristics. The RF signals are mapped to produce a transverse tomographic image with excellent resolution of soft tissue contrast.

The most commonly used pulse sequences produce T1-weighted or T2-weighted images, as readers are familiar with, which have special characteristics.[69] Unlike CT, the signal intensity of a given tissue can change depending on the specific pulse sequence used to generate the image, and relative intensity differences between tissues can change or even reverse with the

use of different sequences.

The most commonly used MR contrast agents are small gadolinium molecular agents that increase the signal intensity of contrast-enhancing structures on T1-weighted images.[69]

2.4.2. Diagnostic protocols

T1-, T2- and T1-weighted postcontrast sequences in axial and dorsal planes are recommended to best define normal anatomy and characterize any pathology. Images in the paramedian plane may also prove useful, although in this plane anatomical symmetry is lost within each image. The excellent anatomical detail and characteristic signal intensities of fluid, blood and vascular and avascular tissue on different MR pulse sequences can be used to characterize many urinary tract pathologies, although biopsy is still very often required for definitive diagnosis.[69]

Using T1W and T2W sequences, the shape, size and structure of the renal parenchyma and the collecting system can be easily

assessed. Consequently, an abnormality of these features can be detected, leading to a diagnosis.

In T2W images, urine provides a natural contrast that overcomes the hypointense bladder wall mucosa. This can be used to identify bladder wall thickenings, irregularities or masses. Cystoliths can be detected as hypointense intraluminal structures of variable shape and size in the dependent portion of the urinary bladder and outlined by hyperintense urine.[73]

Dynamic ureterographic magnetic resonance imaging using a series of 3D fast gradient echo sequences (such as fast SPGR or turbo FLASH) has also been described: these sequences, if acquired immediately after contrast medium injection, allow the assessment of both arterial and renal vascular phase and the distribution of the contrast medium in the various vessels (aorta, renal arteries and veins, caudal vena cava).

The excretory phase is acquired immediately after the injection of contrast medium and allows the morphology and structure of the kidneys and ureters to be anatomically assessed.

In order to evaluate kidneys that have been injected with contrast medium and are therefore appear hyperintense, it is necessary to use sequences with suppression of the periureteral adipose signal, which would otherwise also be hyperintense, obliterating the visibility of the ureters.[74]

Evaluations of vascular and excretory phases are useful in combination to identify complex vasculo-ureteral abnormalities, such as retrocaval ureters or abnormal positions of large vessels.[74]

Static urography is a sequence T2W pulses (fast or turbo spin echo) and is a good addition for evaluating conditions that cause dilation of the renal pelvis and/or ureters or urinomas, as the fluid in these structures will appear hyperintense. Fat saturation

is useful as it increases the visibility of fluid-filled ureters compared to the suppressed signal of retroperitoneal fat.[74] One author reported that 3D Contrast enhanced magnetic resonance angiography (CE-MRA) using multiphase FSGR sequence and elliptical centric k-space ordering is a fast and efficient method to non-invasively image the renal vessels with enough temporal resolution to obtain separate arterial and venous enhancement. These results suggest that CE-MRA could potentially replace contrast-enhanced computed tomography angiography for screening the vascularization of kidneys in donors transplant programs, as previously reported in humans.[73]

These techniques can be particularly useful when renal function is poor, resulting in decreased renal excretion of gadolinium. Various non-contrast techniques have been specifically developed and applied to renal imaging.[75;76] Contras enhanced-MRA uses gadolinium, a paramagnetic contrast agent that increases blood signal and consequently the blood signal is

directly related to concentration of gadolinium and relatively independent of flow dynamics.[70;77]

In human medicine, using gadolinium-based contrast media that are eliminated through glomerular filtration without reabsorption or tubular secretion, researchers have also used dynamic MRI nephrography to measure renal function and provide a morphological assessment of renal structure.[78]

2.5. Renal Scintigraphy

Kidney disease is common in domestic animals, particularly in feline patients. For the diagnosis and monitoring of kidney disease in animals, veterinarians generally rely on clinical signs and blood tests, which are often very non-specific. Moreover, clinical signs and haematobiochemical changes only manifest themselves at a late stage, when renal damage is already advanced. Animals often first present renal disease with a

history of polyuria or polydipsia or both.[6] As in humans, evidence of haematochemical abnormalities, such as creatinine elevations, is not detected until 65-75% of the nephrons have been damaged.[79]

As seen so far, imaging is a fundamental part of the diagnostic procedure for renal disease in veterinary patients.

Renal scintigraphy is performed in dogs and cats and has also been successfully performed in a variety of other species. The availability of renal scintigraphy is extremely limited in veterinary medicine. This is largely due to the cost of nuclear medicine equipment, the requirement for a license to use radioactive materials and the lack of sufficient technical expertise.[79]

2.5.1. Indications

The indications for renal scintigraphy in animals are similar to those in humans. However, the use of renal scintigraphy in combination with advanced treatment procedures, such as renal

transplantation, is much less common due to the low uptake of the latter.

The primary objective of most studies is to determine the overall and fractional renal glomerular filtration rate (GFR).

Renal scintigraphy is most commonly performed in dogs undergoing nephrectomy or nephrotomy and in patients with urolithiasis. Surgery may be necessary to remove a mass involving the kidney, a nidus of infection that cannot be controlled by antibiotics, a chronically hydronephrotic kidney or for nephrolithias. Renal scintigraphy may also be useful for assessing overall renal function in cases of subclinical renal disease. This is particularly important in cases where treatment may lead to a further reduction in renal function, such as when nephrotoxic drugs are administered.[80]

Renal scintigraphy is also commonly performed in cats being evaluated for treatment of hyperthyroidism, with iodine-131, or undergoing nephrectomy.[65]

2.5.2. Technique and Procedure

In clinical veterinary medicine, renal scintigraphy is performed almost exclusively with technetium (99mTc)-diethylenetri-amine penta-acetic acid (DTPA). Renal scintigraphy is often combined with the administration of a diuretic to assess the patency of ureters from obstructive ureterolithiasis or stenosis.[81] 99mTc-DTPA is used as a glomerular filtration agent. The suitability of 99mTc-DTPA for measuring GFR varies between animal species due to protein binding in vivo. If part of the injected dose of 99mTc-DTPA binds to plasma proteins, it would not be available for glomerular filtration and would falsely decrease the measured GFR or affect the ability to visualize renal morphology. In dogs and cats, the protein binding of 99mTc-DTPA is minimal (6%-7%) and does not significantly affect renal absorption.[82] Although 99mTc-DTPA would probably be suitable for most mammalian domestic species, the

amount of protein binding must be ascertained to be species-specific before use in a previously untested species.

For the measurement of renal function and morphology imaging is performed with a delay of 2-3 hours after injection and is necessary to allow adequate time for renal concentration of the radiopharmaceutical uptake. At 4 hours after injection, 51.7% and 2.5% of the radiopharmaceutical binds to the kidney in healthy dogs. The 99mTc-dimercapto-succinic acid (DMSA) can also be used to detect masses that displace renal tubular cells. These lesions appear as photopaque defects.

The 99mTc-DMSA can also be used to quantify relative (left vs. right) functioning renal tubular mass.[83] In a study conducted in dogs subjected to renal tubular damage by toxic doses of gentamicin, the 99mTc-DMSA was able to detect disease earlier than either 99mTc-DTPA.

Renal scintigraphy is also performed in large animals, such as the horse. To improve the quality of the study, motion correction software can be used to compensate for the typical wave-like movement of the horse during the 60-90 second time interval required to acquire the images. Images can be repeated if necessary.

Differential estimation of functioning renal tubular mass can be achieved by establishing the percentage of 99mTc-DMSA dose uptake by the left and right kidneys.[84] It is important to note that this provides an estimate of functioning renal tubular mass and not renal function, as poor DMSA uptake has been observed in patients with renal tubulointerstitial disease in the presence of normal DTPA uptake.

Renal scintigraphy has also been used in various non-traditional companion animals. For example, for the assessment of serum or plasma concentrations of urea nitrogen and creatinine in reptiles, which are not useful indicators of renal failure because

they are not elevated until there is extensive renal damage and are also non-specific because they are also influenced by diet, reproductive status and hydration.[85;86] In avian species, uric acid concentrations are used for the assessment of renal disease, but significant renal dysfunction is required before an increase in uric acid concentration can be observed. Another factor is that uric acid secretion occurs mainly from the proximal tubules and does not reflect the GFR.[87] For this reason, renal scintigraphy has been investigated as a method to better assess renal disease in these species. The 99mTc-DTPA is the method of choice for the assessment of renal function in birds, but the 99mTc-DMSA has been found to be better for the assessment of renal morphology. In snakes, 99mTc-mercaptoacetyltriglycine appears to be better than 99mTc-DTPA or 99mTc-DMSA for the assessment of renal structure and function. In iguanas, 99mTc-DMSA proved useful for the assessment of renal structure and function.

References

1. Robotti G, Lanfranchi D. Urinary tract disease in dogs: US findings. A mini-pictorial essay. J Ultrasound. 2013 May 14;16(2):93-6. doi: 10.1007/s40477-013-0012-2. PMID: 24294350; PMCID: PMC3774912.
2. Forrester SD, Towell TL. Feline idiopathic cystitis. Vet Clin North Am Small Anim Pract. 2015 Jul;45(4):783-806. doi: 10.1016/j.cvsm.2015.02.007. Epub 2015 Mar 23. PMID: 25813400.
3. Byron JK. Urinary Tract Infection. Vet Clin North Am Small Anim Pract. 2019 Mar;49(2):211-221. doi: 10.1016/j.cvsm.2018.11.005. Epub 2018 Dec 24. PMID: 30591189.
4. Hanazono K, Fukumoto S, Endo Y, Ueno H, Kadosawa T, Uchide T. Ultrasonographic findings related to prognosis in canine transitional cell carcinoma. Vet Radiol Ultrasound. 2014 Jan-Feb;55(1):79-84. doi: 10.1111/vru.12085. Epub 2013 Jul 26. PMID: 23890180.
5. Hanazono K, Fukumoto S, Endo Y, Ueno H, Kadosawa T, Uchide T. Ultrasonographic findings related to prognosis in canine transitional cell carcinoma. Vet Radiol Ultrasound. 2014 Jan-Feb;55(1):79-84. doi: 10.1111/vru.12085. Epub 2013 Jul 26. PMID: 23890180.
6. MacLeod A, Wisner E. Computed tomography and magnetic resonance imaging of the urinary tract. In Bartges J, Polzin D, editors: *Nephrology and urology of small animals*, Ames, IA, 2011, Blackwell Publishing.
7. Kyles AE, Hardie EM, Wooden BG, Adin CA, Stone EA, Gregory CR, Mathews KG, Cowgill LD, Vaden S, Nyland TG, Ling GV. Clinical, clinicopathologic, radiographic, and ultrasonographic abnormalities in cats with ureteral calculi: 163 cases (1984-2002). J Am Vet Med Assoc. 2005 Mar 15;226(6):932-6. doi: 10.2460/javma.2005.226.932. PMID: 15786996.
8. Allan G. Radiology in the diagnosis of kidney disease, *Aust Vet Pract* 12:97, 1982.
9. Greco DS. Congenital and inherited renal disease of small animals. Vet Clin North Am Small Anim Pract. 2001 Mar;31(2):393-9, viii. doi: 10.1016/s0195-5616(01)50211-9. PMID: 11265498.

10. Barrett RB, Kneller SK. Feline kidney mensuration. Acta Radiol Suppl. 1972; 319:279-80. PMID: 4531193.
11. Shiroma JT, Gabriel JK, Carter RL, Scruggs SL, Stubbs PW. Effect of reproductive status on feline renal size. Vet Radiol Ultrasound. 1999 May-Jun;40(3):242-5. doi: 10.1111/j.1740-8261.1999.tb00355.x. PMID: 10519301.
12. Park R: Radiology of the urinary bladder and urethra. In O'Brien T, editor: Radiographic diagnosis of abdominal disorders in the dog and cat, Davis, Calif, 1981, Covell Park Veterinary, p 543.
13. Neville-Towle J, Sakals S. Urinary bladder herniation through a caudoventral abdominal wall defect in a mature cat. Can Vet J. 2015 Sep;56(9):934-6. PMID: 26347198; PMCID: PMC4535508.
14. Grand JG, Bureau S, Monnet E. Effects of urinary bladder retroflexion and surgical technique on postoperative complication rates and long-term outcome in dogs with perineal hernia: 41 cases (2002-2009). J Am Vet Med Assoc. 2013 Nov 15;243(10):1442-7. doi: 10.2460/javma.243.10.1442. PMID: 24171374.
15. Mahaffey M, Barber D, Basanti J. Simultaneous double- contrast cystography and cystometry in dogs. Vet Rad and Ultrasound. 2005 May. 25:254–259. Doi: 10.1111/j.1740-8261.1984.tb01940.x
16. Massat BJ, Gregory CR, Ling GV, Cardinet GH, Lewis EL. Cystourethropexy to correct refractory urinary incontinence due to urethral sphincter mechanism incompetence. Preliminary results in ten bitches. Vet Surg. 1993 Jul-Aug;22(4):260-8. doi: 10.1111/j.1532-950x.1993.tb00395. x. PMID: 8351806.
17. Holt P. Urinary incontinence in the bitch due to sphincter mechanism incompetence. J Small Anim Pract. 1985 May; 26:181–190. doi: 10.1111/j.1748-5827.1985.tb02108.x
18. Johnston GR, Osborne CA, Jessen CR, Feeney DA. Effects of urinary bladder distention on location of the urinary bladder and urethra of healthy dogs and cats. Am J Vet Res. 1986 Feb;47(2):404-15. PMID: 3954226.
19. Lobetti RG, Goldin JP. Emphysematous cystitis and bladder trigone diverticulum in a dog. J Small Anim Pract. 1998 Mar;39(3):144-7. doi: 10.1111/j.1748-5827.1998.tb03620.x. PMID: 9551384.

20. Petite A, Busoni V, Heinen MP, Billen F, Snaps F. Radiographic and ultrasonographic findings of emphysematous cystitis in four nondiabetic female dogs. Vet Radiol Ultrasound. 2006 Jan-Feb;47(1):90-3. doi: 10.1111/j.1740-8261.2005.00112. x. PMID: 16429992.
21. Feeney DA, Barber DL, Culver DH, Prasse KW, Thrall DE, Lewis RE. Canine excretory urogram: correlation with base-line measurements. Am J Vet Res. 1980 Feb;41(2):279-83. PMID: 7369601.
22. Burk RL, Feeney DA (ed): Small Animal Radiology and Ultrasonography (ed 3). Philadelphia, W.B. Saunders, 2002, pp 356-359
23. Feeney DA, Johnson GR: The kidneys and ureters, in Thrall DE (ed): Textbook of Veterinary Diagnostic Radiology (ed 3). Philadelphia, PA, Saunders, 1997, pp 466-478
24. Holland M. In: Contrast agents. Vet Clin North Am Small Anim Pract 23:269-279, 1993
25. DiBartola SP. Clinical approach and laboratory evaluation of renal disease, in Ettinger SJ (ed): Textbook of Veterinary Internal Medicine (ed 4). Philadelphia, PA, Saunders, 1995, pp 1706-1719
26. Thomsen HS. European Society of Urogenital Radiology (ESUR) guidelines on the safe use of iodinated contrast media. Eur J Radiol. 2006 Dec;60(3):307-13. doi: 10.1016/j.ejrad.2006.06.020. Epub 2006 Sep 11. PMID: 16965884.
27. Rao QA, Newhouse JH. Risk of nephropathy after intravenous administration of contrast material: a critical literature analysis. Radiology. 2006 May;239(2):392-7. doi: 10.1148/radiol.2392050413. Epub 2006 Mar 16. PMID: 16543592.
28. Ackerman N, Ling GV, Lowenstine LJ, Cowgill LD. Percutaneous nephropyelocentesis and nephropyelostomy in the dog: a description of the technique. Am J Vet Res. 1979 Nov;40(11):1605-12. PMID: 525880.
29. Rivers BJ, Walter PA, Polzin DJ. Ultrasonographic-guided, percutaneous antegrade pyelography: technique and clinical application in the dog and cat. J Am Anim Hosp Assoc. 1997 Jan-Feb;33(1):61-8. doi: 10.5326/15473317-33-1-61. PMID: 8974029.

30. Specchi S, Lacava G, d'Anjou MA, Zini E, Auriemma E. Ultrasound-guided percutaneous antegrade pyelography with computed tomography for the diagnosis of spontaneous partial ureteral rupture in a dog. Can Vet J. 2012 Nov;53(11):1187-90. PMID: 23633712; PMCID: PMC3474574.
31. Oliver JE Jr, Young WO. Air cystometry in dogs under xylazine-induced restraint. Am J Vet Res. 1973 Nov;34(11):1433-5. PMID: 4748727.
32. Feeney DA, Johnston GR, Tomlinson MJ, Osborne CA. Effects of sterilized micropulverized barium sulfate suspension and meglumine iothalamate solution on the genitourinary tract of healthy male dogs after retrograde urethrocystography. Am J Vet Res. 1984 Apr;45(4):730-8. PMID: 6731987.
33. Farrow CS. Exercise in diagnostic radiology. Can Vet J. 1982 Sep;23(9):279-80. PMID: 17422185; PMCID: PMC1790205.
34. Graham J. 2011. BSAVA Manual of Canine and Feline Ultrasonography. Kidneys and proximal ureters Chapter 10 pp 110
35. Mareschal A, d'Anjou MA, Moreau M, Alexander K, Beauregard G. Ultrasonographic measurement of kidney-to-aorta ratio as a method of estimating renal size in dogs. Vet Radiol Ultrasound. 2007 Sep-Oct;48(5):434-8. doi: 10.1111/j.1740-8261.2007.00274.x. PMID: 17899978.
36. Barella G, Lodi M, Sabbadin LA, Faverzani S. A new method for ultrasonographic measurement of kidney size in healthy dogs. J Ultrasound. 2012 Sep;15(3):186-91. doi: 10.1016/j.jus.2012.06.004. Epub 2012 Jul 2. PMID: 23459261; PMCID: PMC3558091.
37. Bua AS, Dunn ME, Pey P. Respective associations between ureteral obstruction and renomegaly, urine specific gravity, and serum creatinine concentration in cats: 29 cases (2006-2013). J Am Vet Med Assoc. 2015 Sep 1;247(5):518-24. doi: 10.2460/javma.247.5.518. PMID: 26295557.
38. D'Anjou MA, Bédard A, Dunn ME. Clinical significance of renal pelvic dilatation on ultrasound in dogs and cats. Vet Radiol Ultrasound. 2011 Jan-Feb;52(1):88-94. PMID: 21322393.

39. Debruyn K, Paepe D, Daminet S, Combes A, Duchateau L, Peremans K, Saunders JH. Comparison of renal ultrasonographic measurements between healthy cats of three cat breeds: Ragdoll, British Shorthair and Sphynx. J Feline Med Surg. 2013 Jun;15(6):478-82. doi: 10.1177/1098612X12471057. Epub 2012 Dec 12. PMID: 23234720.
40. Yeager AE, Anderson WI. Study of association between histologic features and echogenicity of architecturally normal cat kidneys. Am J Vet Res. 1989 Jun;50(6):860-3. PMID: 2475043.
41. Hart DV, Winter MD, Conway J, Berry CR. Ultrasound appearance of the outer medulla in dogs without renal dysfunction. Vet Radiol Ultrasound. 2013 Nov-Dec;54(6):652-8. doi: 10.1111/vru.12069. Epub 2013 Jun 6. PMID: 23738847.
42. Wilson HM, Chun R, Larson VS, Kurzman ID, Vail DM. Clinical signs, treatments, and outcome in cats with transitional cell carcinoma of the urinary bladder: 20 cases (1990-2004). J Am Vet Med Assoc. 2007 Jul 1;231(1):101-6. doi: 10.2460/javma.231.1.101. Erratum in: J Am Vet Med Assoc. 2007 Nov 15;231(10):1533. PMID: 17605672.
43. Ettinger SJ, Feldman EC. Textbook of veterinary internal medicine: Diseases of the dog and the cat. St. Louis: Elsevier; 2017:2069.
44. Finn-Bodner ST (1995) The urinary bladder. In: Cartee RE, Selcer BA, Hudson JA et al., eds. Practical Veterinary Ultra- sound. Philadelphia: Lea and Febiger, pp 210–235.
45. Geisse AL, Lowry JE, Schaeffer DJ, Smith CW. Sonographic evaluation of urinary bladder wall thickness in normal dogs. Vet Radiol Ultrasound. 1997 Mar-Apr;38(2):132-7. doi: 10.1111/j.1740-8261.1997.tb00828.x. PMID: 9238782.
46. Oh H, Kim S, Kim S, Lee J, Yun S, Yoon J, Jung J, Choi M. Evaluation of the ureteral jet in dogs by using color Doppler ultrasonography. J Vet Sci. 2017 Sep 30;18(3):399-406. doi: 10.4142/jvs.2017.18.3.399. PMID: 28057900; PMCID: PMC5639093.
47. Caruso G, Salvaggio G, Campisi A, et al. Bladder tumor staging: comparison of contrast-enhanced and Gray-Scale Ultrasound. American Journal of Roentgenology 2010; 194: 151–156.

48. Pollard RE, Watson KD, Hu X, Ingham E, Ferrara KW. Feasibility of quantitative contrast ultrasound imaging of bladder tumors in dogs. Can Vet J 2017; 58: 70–72.
49. Haers H, Vignoli M, Paes G, Rossi F, Taeymans O, Daminet S, Saunders JH. Contrast harmonic ultrasonographic appearance of focal space-occupying renal lesions. Vet Radiol Ultrasound. 2010 Sep-Oct;51(5):516-22. doi: 10.1111/j.1740-8261.2010.01690. x. PMID: 20973385.
50. Barthez PY, Begon D, Delisle F. Effect of contrast medium dose and image acquisition timing on ureteral opacification in the normal dog as assessed by computed tomography. Vet Radiol Ultrasound. 1998 Nov-Dec;39(6):524-7. doi: 10.1111/j.1740-8261. 1998.tb01643.x. PMID: 9845189.
51. Rozear L, Tidwell AS. Evaluation of the ureter and ureterovesicular junction using helical computed tomographic excretory urography in healthy dogs. Vet Radiol Ultrasound. 2003 Mar-Apr;44(2):155-64. doi: 10.1111/j.1740-8261. 2003.tb01264.x. PMID: 12718349.
52. Longo M, Andreis ME, Pettinato C, Ravasio G, Rabbogliatti V, De Zani D, Di Giancamillo M, Zani DD. Use of the bolus tracking technique for the tomographic evaluation of the uretero-vesicular junction in dogs and assessment of dose records. BMC Vet Res. 2016 Mar 29;12:64. doi: 10.1186/s12917-016-0690-z. PMID: 27026013; PMCID: PMC5477813.
53. O'Dell-Anderson KJ, Twardock R, Grimm JB, Grimm KA, Constable PD. Determination of glomerular filtration rate in dogs using contrast-enhanced computed tomography. Vet Radiol Ultrasound. 2006 Mar-Apr;47(2):127-35. doi: 10.1111/j.1740-8261.2006.00118.x. PMID: 16553143.
54. Gaspari F, Perico N, Remuzzi G. Application of newer clearance techniques for the determination of glomerular filtration rate. Curr Opin Nephrol Hypertens. 1998 Nov;7(6):675-80. doi: 10.1097/00041552-199811000-00009. PMID: 9864664.
55. Miyamoto K. Use of plasma clearance of iohexol for estimating glomerular filtration rate in cats. Am J Vet Res. 2001 Apr;62(4):572-5. doi: 10.2460/ajvr.2001.62.572. PMID: 11327466.

56. Finco DR, Braselton WE, Cooper TA. Relationship between plasma iohexol clearance and urinary exogenous creatinine clearance in dogs. J Vet Intern Med. 2001 Jul-Aug;15(4):368-73. PMID: 11467595.
57. Finco DR, Coulter DB, Barsanti JA. Simple, accurate method for clinical estimation of glomerular filtration rate in the dog. Am J Vet Res. 1981 Nov;42(11):1874-7. PMID: 7337283.
58. Watson AD, Lefebvre HP, Concordet D, Laroute V, Ferré JP, Braun JP, Conchou F, Toutain PL. Plasma exogenous creatinine clearance test in dogs: comparison with other methods and proposed limited sampling strategy. J Vet Intern Med. 2002 Jan-Feb;16(1):22-33. doi: 10.1892/0891-6640(2002)016<0022:peccti>2.3.co;2. PMID: 11826881.
59. Dawson P, Peters M. Dynamic contrast bolus computed tomography for the assessment of renal function. Invest Radiol. 1993 Nov;28(11):1039-42. doi: 10.1097/00004424-199311000-00014. PMID: 8276575.
60. Tsushima Y. Functional CT of the kidney. Eur J Radiol. 1999 Jun;30(3):191-7. doi: 10.1016/s0720-048x(99)00011-x. PMID: 10452717.
61. Miles KA, Leggett DA, Bennett GA. CT derived Patlak images of the human kidney. Br J Radiol. 1999 Feb;72(854):153-8. doi: 10.1259/bjr.72.854.10365065. PMID: 10365065.
62. Tsushima Y, Blomley MJ, Kusano S, Endo K. Use of contrast-enhanced computed tomography to measure clearance per unit renal volume: a novel measurement of renal function and fractional vascular volume. Am J Kidney Dis. 1999 Apr;33(4):754-60. doi: 10.1016/s0272-6386(99)70230-1. PMID: 10196020.
63. Mori S, Yashiro H, Inoue M, Takahara K, Kusaka M, Shiroki R. Urodynamic 4D-CT evaluation: 320-row area detector CT scanner combined with PhyZiodynamics software analysis provides an innovative system to evaluate urinary flow and outlet obstructions. Acta Radiol. 2020 Apr;61(4):558-567. doi: 10.1177/0284185119868909. Epub 2019 Aug 25. PMID: 31446779.
64. Cáceres AV, Zwingenberger AL, Aronson LR, Mai W. Characterization of normal feline renal vascular anatomy with dual-

phase CT angiography. Vet Radiol Ultrasound. 2008 Jul-Aug;49(4):350-6. doi: 10.1111/j.1740-8261.2008.00378.x. PMID: 18720765.
65. Tyson R, Daniel GB. Renal scintigraphy in veterinary medicine. Semin Nucl Med. 2014 Jan;44(1):35-46. doi: 10.1053/j. PMID: 24314044.
66. Hoey SE, Heder BL, Hetzel SJ, Waller KR 3rd. Use of computed tomography for measurement of kidneys in dogs without renal disease. J Am Vet Med Assoc. 2016 Feb 1;248(3):282-7. doi: 10.2460/javma.248.3.282. PMID: 26799106.
67. Lane IF, Lappin MR, Seim HB 3rd. Evaluation of results of preoperative urodynamic measurements in nine dogs with ectopic ureters. J Am Vet Med Assoc. 1995 May 1;206(9):1348-57. PMID: 7775247.
68. Cronin RE. Contrast-induced nephropathy: pathogenesis and prevention. Pediatr Nephrol. 2010 Feb;25(2):191-204. doi: 10.1007/s00467-009-1204-z. Epub 2009 May 15. PMID: 19444480.
69. Mai W. Diagnostic MRI in dog and cat. © 2018. In: Taylor & Francis Group, LLC Edited by W Mai. Chapter 10. Pp 743
70. Prince MR, Meaney JF. Expanding role of MR angiography in clinical practice. Eur Radiol. 2006 Feb;16 Suppl 2:B3-8. doi: 10.1007/s10406-006-0161-x. PMID: 16802437.
71. Thornton J, O'Callaghan J, Walshe J, O'Brien E, Varghese JC, Lee MJ. Comparison of digital subtraction angiography with gadolinium-enhanced magnetic resonance angiography in the diagnosis of renal artery stenosis. Eur Radiol. 1999;9(5):930-4. doi: 10.1007/s003300050769. PMID: 10369993.
72. Glockner JF, Vrtiska TJ. Renal MR and CT angiography: current concepts. Abdom Imaging. 2007 May-Jun;32(3):407-20. doi: 10.1007/s00261-006-9066-3. Epub 2006 Sep 2. PMID: 16952021.
73. Cavrenne R, Mai W. Time-resolved renal contrast-enhanced MRA in normal dogs. Vet Radiol Ultrasound. 2009 Jan-Feb;50(1):58-64. doi: 10.1111/j.1740-8261.2008.01490. x. PMID: 19241755.
74. Duconseille AC, Louvet A, Lazard P, Valentin S, Molho M. Imaging diagnosis--left retrocaval ureter and transposition of the caudal vena

cava in a dog. Vet Radiol Ultrasound. 2010 Jan-Feb;51(1):52-6. doi: 10.1111/j.1740-8261.2009.01621.x. PMID: 20166394.
75. Maki JH, Wilson GJ, Eubank WB, Glickerman DJ, Millan JA, Hoogeveen RM. Navigator-gated MR angiography of the renal arteries: a potential screening tool for renal artery stenosis. AJR Am J Roentgenol. 2007 Jun;188(6):W540-6. doi: 10.2214/AJR.06.1138. PMID: 17515344.
76. Wielopolski PA, Adamis M, Prasad P, Gaa J, Edelman R. Breath-hold 3D STAR MR angiography of the renal arteries using segmented echo planar imaging. Magn Reson Med. 1995 Mar;33(3):432-8. doi: 10.1002/mrm.1910330319. PMID: 7760713.
77. Kuriashkin IV, Losonsky JM. Contrast enhancement in magnetic resonance imaging using intravenous paramagnetic contrast media: a review. Vet Radiol Ultrasound. 2000 Jan-Feb;41(1):4-7. doi: 10.1111/j.1740-8261. 2000.tb00419.x. PMID: 10695873.
78. Fonseca-Matheus JM, Pérez-García CC, Ginja MM, Altónaga JR, Orden MA, Gonzalo-Orden JM. Contrast-enhanced dynamic magnetic resonance nephrography in healthy dogs. Vet J. 2011 Sep;189(3):341-5. doi: 10.1016/j.tvjl.2010.06.025. Epub 2010 Aug 31. PMID: 20810295.
79. LeFebvre HP: Renal function testing. In: Bartges J, Polzin DJ, (eds): Nephrology and Urology of Small Animals. Ames, IA: John Wiley & Sons; 2011
80. Daniel G, Hahn K, Bravo L, Legendre A. The effect of a single therapeutic dose of cisplatin on GFR in dogs. Oncol Rep. 1997 Jan-Feb;4(1):153-6. PMID: 21590032.
81. Hecht S, Lawson SM, Lane IF, Sharp DE, Daniel GB. (99m)Tc-DTPA diuretic renal scintigraphy in dogs with nephroureterolithiasis. Can Vet J. 2010 Dec;51(12):1360-6. PMID: 21358928; PMCID: PMC2978988.
82. Krawiec DR, Badertscher RR 2nd, Twardock AR, Rubin SI, Gelberg HB. Evaluation of 99mTc-diethylenetriaminepentaacetic acid nuclear imaging for quantitative determination of the glomerular filtration rate of dogs. Am J Vet Res. 1986 Oct;47(10):2175-9. PMID: 3777642.
83. Lora-Michiels M, Anzola K, Amaya G, Solano M. Quantitative and qualitative scintigraphic measurement of renal function in dogs

exposed to toxic doses of Gentamicin. Vet Radiol Ultrasound. 2001 Nov-Dec;42(6):553-61. doi: 10.1111/j.1740-8261.2001.tb00986.x. PMID: 11768525.

84. Morton KA, Clarke PB, Boldgett TM, et al: Genitourinary. In: Morton KA, Clarke PB, (eds): Diagnostic Imaging: Nuclear Medicine. Salt Lake City: Amirsys; 2007
85. Greer LL, Daniel GB, Shearn-Bochsler VI, Ramsay EC. Evaluation of the use of technetium Tc 99m diethylenetriamine pentaacetic acid and technetium Tc 99m dimercaptosuccinic acid for scintigraphic imaging of the kidneys in green iguanas (Iguana iguana). Am J Vet Res. 2005 Jan;66(1):87-92. doi: 10.2460/ajvr.2005.66.87. PMID: 15691041.
86. Sykes JM 4th, Schumacher J, Avenell J, Ramsay E, Daniel GB. Preliminary evaluation of 99mTechnetium diethylenetriamine pentaacetic acid, 99mTechnetium dimercaptosuccinic acid, and 99mTechnetium mercaptoacetyltriglycine for renal scintigraphy in corn snakes (Elaphe guttata guttata). Vet Radiol Ultrasound. 2006 Mar-Apr;47(2):222-7. doi: 10.1111/j.1740-8261.2006.00131.x. PMID: 16553157.
87. Marshall KL, Craig LE, Jones MP, Daniel GB. Quantitative renal scintigraphy in domestic pigeons (Columba livia domestica) exposed to toxic doses of gentamicin. Am J Vet Res. 2003 Apr;64(4):453-62. doi: 10.2460/ajvr.2003.64.453. PMID: 12693536.

3. RESEARCH PAPERS

3.1. **Paper one:** Fall time may be a reliable discriminator between neoplastic and non-neoplastic urinary bladder lesions in dogs undergoing Contrast-Enhanced Ultrasound: a pilot study

Carlotta Spediacci [1], Martina Manfredi [1], Giulia Sala [1], Tiziana Liuti [2], Nicolas Israeliantz [2] , Davide Danilo Zani [1], Mauro Di Giancamillo [1], Maurizio Longo [1]

[1] Departement of Veterinary Medicine, University of Milan, Street of University n. 6, 26900, Lodi (LO), Italy
[2] Royal Dick School of Veterinary Studies, University of Edinburgh, Edinburgh, Scotland, UK

Corresponding author: Carlotta Spediacci (carlotta.spediacci@unimi.it)

Key Words: *Canine, Neoplasia, Polypoid cystitis, Bladder Disease, Quantitative CEUS*
Conflict of Interest: the authors declare that there is no financial interest related to article content.

Abstract

Contrast-enhanced ultrasound (CEUS) can provide quantitative information on enhancement patterns and perfusion of lesions, based on time-intensity curves (TICs). No published studies have compared CEUS parameters in neoplastic and non-neoplastic urinary bladder lesions in dogs. A prospective, pilot study was conducted to quantitatively characterize the CEUS pattern of neoplastic and non-neoplastic urinary bladder lesions in dogs, assessing the influence of contrast arrival time (CAT) on the final appearance of the curves. Fourteen dogs with cyto-histopathological diagnoses were prospectively included (seven malignant and seven inflammatory lesions). B-mode ultrasound was performed followed by CEUS examination after an intravenous bolus injection of 0.04 mL/kg of contrast medium, and TICs were elaborated by dedicated software. Receiver operating characteristic curves (ROC) for each TIC parameter were obtained. Neoplastic lesions presented subjectively shorter

rise time (RT), time to peak (TTP) and fall time (FT) than the inflammatory disease. Based on ROC curve analyses, fall time ≥ 10.49 s was the most reliable parameter in diagnosing non-neoplastic disease in this group of dogs (area under the curve [AUC] 0.75, sensitivity 83.33%, specificity 66.67%). No difference was found between ROCs calculated for each parameter of TICs by adding or removing CAT. The results suggest that neoplastic and non-neoplastic diseases are characterized by different TICs and can be used as background for the future. However, larger scale studies are needed evaluating use of CEUS FT threshold of 10.49 s as a possible discriminator for urinary bladder lesions in dogs. Thus, biopsy is still recommended for a final diagnosis.

Introduction

Urinary bladder neoplasms account for approximately 1–2% of all malignant tumors in dogs.[1] Epithelial tumors are the most

common, representing approximately 97% of all malignant neoplasms, including urothelial cell carcinoma (UCC), followed by squamous cell carcinoma and adenocarcinoma.[2] Other less common neoplasms of non-epithelial origins are leiomyoma, leiomyosarcoma, fibroma, hemangioma, hemangiosarcoma, and lymphoma.[3-5] The urinary bladder is also frequently affected by non-neoplastic pathologies, such as urolithiases and cystitis.[6;7] Common clinical signs include hematuria, stranguria, and other forms of dysuria. Additionally, in dogs affected by neoplastic conditions, lameness, weight loss, and lethargy are rarely reported.[5] Diagnostic ultrasonography (US) is a standard diagnostic imaging test for dogs with suspected urinary bladder neoplasia. This is due to its ease of use, low cost, and excellent real-time contrast resolution.[8] Demhiwall et al. described thickening of the bladder wall as the most common US finding in inflammatory diseases of the urinary tract. Similar findings were also observed by other authors.[9;10] Polypoid cystitis in

particular, with mass-like mucosal proliferation and severe diffuse bladder wall thickening, may present overlapping characteristics with urinary neoplasia. On US, UCC is characterized by an intramural infiltration with high vascularization, and most frequently affect the bladder trigone.[9;11-14] Urinary bladder polyps may show similar characteristics, with pedunculated mural masses often multifocal in distribution.[15;16] Moreover, US shows low specificity in differentiating between benign and malignant bladder lesions.[17]

Definitive diagnosis for urinary neoplasms in dogs requires invasive tests such as transcutaneous fine-needle aspiration, cystotomy, cystoscopy-guided biopsies, or traumatic catheterization. Furthermore, transcutaneous procedures are discouraged due to the risk of tumor seeding.[5;18]

A quantitative, ultrasonographic method for discriminating neoplastic versus non-neoplastic urinary bladder masses would therefore be helpful for improving prognosis and treatment planning in affected patients. Previous studies in dogs have described the use of CEUS for the detection of splenic and hepatic malignancies in pets. However, both quantitative and qualitative analyses of CEUS of the lower urinary tract are poorly described in veterinary medicine, with a recent study focusing on UCC in a limited cohort of canine patients.[30] The authors described a vivid enhancement of the neoplasms, with rapid wash-in and a slower wash-out phase, with loss of wall layering. In human medicine, the extent of angiogenesis in malignant neoplasms of the urinary bladder has been reported to be associated with tumor growth and metastasis formation and CEUS is considered useful for the diagnosis of urinary bladder neoplasia. [19-23] The differentiation of neoplastic and non-neoplastic lesions of urinary bladder might be performed

quantifying the CEUS pattern derived from time-intensity curves (TICs). [27] A thorough evaluation of both the urinary bladder layers and tumoral angiogenesis is essential to establish the degree of aggressiveness of the urinary bladder neoplasms and thus to define an accurate prognosis. [39] The close analogy between canine and human urothelial cell carcinoma has been demonstrated in numerous studies, making the dog an animal model for studying this disease. [40]

The use of CEUS may represent an important ancillary technique in daily practice, particularly in the case of challenging bioptic procedures. These contrast agents consist of gas microbubbles encapsulated by a shell of different compositions.[23] The gas core makes the microbubbles highly echogenic such that each bubble can be ultrasonographically detectable.[24] Most US contrast agents do not diffuse across the endothelium and therefore remain strictly within the vasculature

and microvasculature, allowing accurate assessment of vascular perfusion.[1-28] Following this, the gas content of the contrast agent is eliminated through the lungs, which represents a safe route of clearance, with short-time adverse events occurring in only 0.2% of dogs and cats.[25-26] The CEUS TIC is a quantitative analysis made using perfusion software, which analyzes the temporal sequence of images by measuring the change in pixel intensity in the region of interest (ROI). The signal intensity of each pixel over time is evaluated within the ROI. The final result of this process is a Gaussian curve that quantitatively describes the wash-in and wash-out phases of enhancement.[2-4;19;29;31] The most important quantitative parameters to be considered are the time to peak (TTP), which measures the time from contrast injection to maximum signal intensity (SI); rise time (RT), from the increase of contrast enhancement to SI; Fall Time (FT), indicating the time that the signal takes to return from the peak enhancement to the baseline level; and mean transit time (mTT),

which is defined as the total flow time of the contrast agent in the selected tissue (VueBox Quantification Toolbox, Instruction for use, Copyright 2019 Bracco Suisse SA).[29; 31-21] Another important parameter is the contrast arrival time (CAT), which indicates the time before the appearance of the first microbubble in the selected ROI. The CAT, which represents the first part of the curve, might be automatically removed by the software.[29]

Based on our review of the literature, there were no published studies comparing quantitative CEUS perfusion parameters between neoplastic and non-neoplastic lesions of the urinary bladder in dogs. This study therefore aimed to quantitatively characterize neoplastic and non-neoplastic lesions of the urinary bladder in dogs on CEUS, assessing the influence of CAT on the final appearance of the curves. We firstly hypothesized that CEUS TIC measures previously used for humans with urinary bladder neoplasia would be feasible for use in dogs and that a

cut-off value for some of these measures could be identified for predicting neoplasia versus non-neoplasia in dogs. The second hypothesis was that CAT would represent a highly variable parameter between canine patients of different body conformation, and that this might influence the TIC when not excluded from analyses.

Material and Methods

Experimental design and subject selection criteria:

This was a prospective pilot study. Procedures were approved by the Veterinary Ethics and Welfare Committee of the Royal School of Veterinary Studies of the University of Edinburgh (VERC approval 131.17). Informed owner consent was also obtained before enrollment of the dogs in the study. Dogs presenting to the Hospital for Small Animals at the University of Edinburgh between March 2018 and September 2019 for further investigation of lower urinary tract signs with urinary

bladder changes visible on US were considered. Cases with ultrasonographic diagnosis of urinary bladder mural lesion in which a definitive diagnosis was reached based on histopathology, cytopathology, or microbiology were included. Dogs were excluded from the study if there was evidence of underlying heart disease or if excessive stress was induced by the procedure. All decisions regarding participant inclusion or exclusion criteria were made by an ECVDI board-certified radiologist (TL). The following clinical data were recorded for each dog by a third-year resident (ML): breed, sex, age, weight, and clinical signs. Dogs were divided into three categories according to weight: small (1–10 kg), medium (11–30 kg), and large (>30 kg).

Image acquisition techniques:

All CT examinations were performed by an ECVDI third-year resident (ML) supervised by an ECVDI board-certified veterinary radiologist (TL), who were aware of signalment and

clinical signs of the patients. All dogs also underwent a standardized B-mode US examination of the lower urinary tract (Esaote MyLab Twice, Genova, Italy) using multi-frequency (10–19 MHz) linear (LA435) and micro convex (SC3123) electronic array probes. All dogs were sedated and placed in right lateral recumbency. A small area in the caudal abdomen was clipped to avoid artifacts originating from the hair-coat. The probe was placed in the long axis just cranial to the pelvic inlet and perpendicular to the skin within the ventral midline in females and on the side of the prepuce in males. A layer of gel was applied between the probe and the skin of the patient to obtain good contact with the transducer. The focal point was placed on the urinary bladder wall. For each examination, the presence or absence of lesions, distribution, echotexture, bladder wall thickening, presence of urolithiasis, or urinary sediment were recorded.

Following the B-mode study, a contrast-enhanced ultrasound (CEUS) examination was performed using a contrast-tuned imaging module (CnTI^{TM}, Contrast Tuned Imaging Technology). CEUS was performed using an electronic array probe with a contrast agent capability (SC3123). The lowest gain was set in order to highlight the contrast within the ROI.

A low mechanical index was used and selective placement of the focal zones to maximize the harmonic signal while minimizing the destruction of the contrast media were performed. The mechanical index was 0.3, and only one focal zone was analyzed, which was placed on the urinary bladder wall. The position of the patient and operators were not modified.

The contrast agent (sulfur-hexafluoride echo-signal enhancer, SonoVue®, Bracco Imaging, Milan, Italy) was administered manually in a rapid single bolus at a dosage of 0.04 mL/kg via injection into a direct access port connected to the IV catheter

(20–22 G) placed in the cephalic vein. Each bolus was followed by a flush consisting of 2 mL of saline solution (0.9%).

The occurrence of adverse events was evaluated and recorded by a single observer (NI). Potential systemic side effects were monitored during sedation; cardiovascular and pulmonary parameters were monitored and reported in the anaesthesia report; any unpredictable changes were reported.

Image analyses

After administration of CEUS, for each dog a qualitative evaluation was performed by assessing the type of enhancement, that was defined as mild, moderate or marked and homogeneous or heterogeneous (Fig. 6), in agreement among the three observers who were blinded to final diagnosis (ML, TL, NI).

During each examination, a 2-min digital video clip was recorded from the time of contrast injection. All raw data were stored in a local picture archiving and communication system and subsequently analyzed by three blinded observers (ML,

TL, NI). Results with the highest Quality of Fit of the curves for each patient were recorded. Post-processing quantitative analysis of the video clips was performed using image-analysis software (Vue Box®, Bracco Imaging, Milan, Italy). For each dog, a ROI was drawn at the center of the lesion of interest. The ROI was drawn individually for each patient, selecting the smaller size and the most representative shape to avoid the inclusion of non-representative peripheral tissues (Fig. 7). Furthermore, for each ROI, a TIC perfusion model was elaborated by extrapolating the following data: SI, TTP, RT mTT, and FT. Each parameter was plotted in an Excel file sheet; afterward, each value was added to the CAT and also reported in the Excel file (Microsoft Excel 365, 2020 16.43 [20110804]).

Statistical Analyses

All statistical analyses were performed by a clinical statistician (GS) using dedicated software (SPSS 26.0, Mac IBM, Armonk,

USA). Because of the small sample, data were analyzed by using descriptive rather than inferential statistics. Descriptive statistics were produced, and continuous variables were expressed as mean ± standard deviation (SD), while categorical variables were expressed as frequencies and percentages with 95% confidence intervals.

Power analysis was performed with the G-power software using an alpha-error of 0.05 and a sample effect of 0.5.

Receiver operating characteristic (ROC) curve was performed for each CEUS parameter (SI, TTP, RT mTT, and FT with and without CAT). The ROC was built to establish the optimal cut-off value associated with neoplastic or non-neoplastic lesions. The optimal cut-off point was chosen using the Youden index, where sensitivity and specificity were maximized, and equal weight was given to false-positive and false-negative results. The calculated cut-off values were used to calculate sensitivity and specificity. Additionally, the area under the curve (AUC)

and 95% confidence intervals (CI) were calculated and used as indicators of the accuracy of the parameters. [33] Interpretation of AUC was based on the following scoring system: 1.0 perfect test, 0.99–0.90 excellent test, 0.89–0.80 good test, 0.79–0.70 fair test, 0.69–0.51 poor test, and 0.50 or lower fail. [33]

Results

Fourteen canine patients of different sexes, weights, and breeds met the inclusion criteria. Ten were female and four were male; the mean weight was 15.3 ± 9.4 kg, and the mean age was 8.5 ± 3.5 years. Two dogs were classified as large, three as small, and nine as medium size. Represented breeds were one of the following: cattle dogs, Chinese crested, Labrador Retriever, Lakeland Terrier, mixed breed, Norfolk Terrier, Podenco Canario, Schnauzer, Scottish Terrier, West Highland White Terrier, Weimaraner, Border Collie, and two Cocker Spaniels. The recorded clinical signs were hematuria, pollakiuria, and

stranguria, and nocturia, and urinary incontinence in one case. In the neoplastic group, the definitive diagnosis was always obtained on the basis of a positive cytological examination performed by traumatic catheterization. In the non-neoplastic group, diagnosis was performed by cystoscopy guided biopsy in one case (polypoid cystitis), traumatic catheterization in one case (dysplasia of epithelial cell), and in five cases the final diagnosis was made on the basis of cystocentesis and microbiological cultural examination.

Inflammatory lesions not cytologically-histologically confirmed were clinically monitored with a complete resolution of the clinical signs and a normal one month follow up ultrasound.

Histological and cytological analysis revealed seven neoplastic lesions (UCC) and seven inflammatory diseases (one dysplasia of epithelial cell, one polypoid cystitis, four bacterial cystitis, and one cystolithiasis). In both the neoplastic and non-neoplastic groups, five dogs were female and two were male. B-mode US

findings of neoplastic lesions were irregular thickening of the bladder wall with loss of normal layering and pedunculated round-shaped masses, sometimes mineralized, located at the level of the urinary bladder trigone. US B-mode of dogs with non-neoplastic conditions showed generalized thickening of the bladder wall, polypoid masses, and in one case, hydroureter, hydronephrosis, and cystolithiasis were also detected. In all cases, the normal portion of the urinary bladder wall was identified as two parallel hyperechoic thin layers and a hypoechoic interposed layer that corresponded to the muscular layer.

Qualitative analysis of CEUS in neoplastic lesions showed moderate (4 of 7) to marked (3 of 7) and heterogeneous enhancement (7 of 7), with the presence of multiple non-enhancing central areas likely compatible with necrosis. In two dogs of the neoplastic group only irregular thickening of the wall bladder was visible (Fig. 1). In these cases, assessing the CEUS

pattern was challenging, given the ill-defined margins of the lesion. In non-neoplastic lesions, a mild (4 of 7) to moderate (1 of 7) and homogeneous (5 of 7) CEUS pattern was visible, with two cases showing mild thickening of the urinary bladder wall and absent enhancement (Fig. 2).

Contrast arrival time was highly variable between individuals, ranging between 2–29.5 s. The mean value of CAT in small dogs was 8 s, in medium-sized dogs was 10.16 s, and in large dogs was 17.3 s (Table 3).

Statistical comparison between the groups was not performed due to small sample sizes, but descriptive analyses of the quantitative parameters displayed neoplastic lesions with subjectively shorter RT, TTP, FT and longer mTT compared to inflammatory lesions (Fig. 3) (Table 1). From the analysis of the ROC curves (Table 2), FT ≥ 10.49 s proved to be the most accurate parameter in diagnosing non-neoplastic disease (AUC 0.75, sensitivity 83.33%, specificity 66.67%). Moreover, RT ≥

6.75 s and TTP ≥ 9.94 s were both indicative of a non-neoplastic etiology (AUC 0.595, sensitivity 66.67%, specificity 71.43%). The AUC tested for the remaining parameters failed to differentiate between neoplastic and non-neoplastic lesions (Table 2). No difference was found between the ROC analysis for each parameter by adding or removing CAT. Only the values without CAT were considered as relevant and reported in table 1 and 2. No immediate or delayed adverse reaction was detected during the examination.

Discussion

The quantitative CEUS parameters of neoplastic and non-neoplastic lesions of the urinary bladder in canine patients were investigated. Among the analyzed parameters, only FT was found to be potentially useful for distinguishing neoplastic and non-neoplastic lesions of the urinary bladder. No other parameters were distinctive for neoplastic and non-neoplastic

lesions of the urinary bladder. The second hypothesis related to the influence of CAT in the evaluation of TICs was not supported.

The ROC analyses demonstrated that FT was the most sensitive and specific parameter of the TIC in distinguishing neoplastic and non-neoplastic conditions, with 10.49 s as a cut-off to discriminate between the two groups. As shown in Table 1, the FT averages of neoplastic and non-neoplastic groups differed (10.6 s and 22.24 s, respectively).

In the box plot the distribution of both groups is wide, particularly in the non-neoplastic group (Fig. 4). Moreover, results are not normally distributed, with one outlier in the neoplastic group, which can be expected in a pilot study with a small sample size. Additionally, the ROI selection was challenging in cases without evidence of a well-defined protruding mass, potentially altering the results, such as in patients with non-polypoid cystitis (Fig. 2). A sensitivity and

specificity of 75% has a limited usefulness in a clinical setting. However, median values of the two groups were different, suggesting that this value may potentially be of interest in a study with a larger population.

The CAT parameter was highly variable between individuals of different sizes. However, analysis of the ROC curves did not reveal a decrease in the sensitivity and specificity of any of the TIC parameters, including or removing the CAT value. This may be related to the over-representation of medium-sized dogs in our sample (9/14). The advantage of the software that does not take CAT into account when processing TICs may not have been detected in this study; however, it might be more evident in a population with a larger representation of toy/small and large/giant breeds, with a significantly longer or shorter CAT due to the related anatomical differences influencing contrast medium kinematics.

In veterinary medicine, few studies have evaluated the use of quantitative CEUS TICs for urinary bladder lesions. Pollard et al. reported that CEUS is a feasible technique for the evaluation of the lower urinary tract in dogs: in the cited study, a different contrast agent was used. However, no correlation between CEUS findings, vascular endothelial growth factor concentration, and criteria for assessing response to chemotherapy was found.[32] Another recently published study, which aimed to describe the use of both qualitative and quantitative CEUS of UCC, reported that qualitative perfusion pattern analysis is more reliable than quantitative parameters to reach a definitive diagnosis as the US enhancement measurement might be influenced by many variables, such as cardiac output, blood pressure, and respiratory rate.[30]

In our study qualitative analysis of CEUS pattern showed a moderate to marked heterogeneous enhancement of the neoplastic lesion, in accordance with previous reports. [30] A

heterogeneous CEUS pattern is therefore more indicative of neoplastic infiltration while contrast intensity is overlapping between neoplastic and inflammatory lesions. In this group of dogs, the TIC shape of neoplastic and non-neoplastic lesions was different. The development of easily accessible techniques that allow objective quantification of vascular patterns, such as quantitative CEUS, might be beneficial for the early differentiation of neoplastic and inflammatory lesions of the urinary bladder. The small sample size of this study limited our ability to evaluate predisposition of breed, sex, and age or to compare findings with the previous literature. However, in accordance with previous studies, UCC appeared to be the most common in our sample, as it represented all tumors included in the study.[29-31] Additionally, dogs with neoplastic diseases included predisposed breeds, such as West Highland White Terrier, Scottish Terrier, and Cocker Spaniel.[17;22;34;35-36] Transurethral cystoscopy biopsy could be considered the

preferred diagnostic method in females; however, in male dogs, this method has been reported to be accurate in only 65% of cases.[37] Urine cytology can lead to numerous false-positive and false-negative results, while percutaneous biopsies have been shown to increase the risk of needle-track implantation; therefore, many authors recommend traumatic urethral catheterization to obtain a cytologic diagnosis of UCC.[5;15;17;38]

The first limitation of this study is the small sample size, which did not allow us to reliably define cut-offs for each TIC parameter. Indeed, the power analysis with our sample was 14%, which is limited for a comparison between groups. The choice of selecting ROIs based on bladder lesions appearance meant that different depths were used, and this may have affected the SI, altering the results. Additionally, in cases of thin urinary bladder mural lesions the ROI selection proved to be particularly challenging. Furthermore, the sample was not heterogeneous in terms of patient size; therefore, it was not possible to adequately

investigate the influence of CAT on the accuracy of the curves. Another limitation is the failure to consider heart rate and blood pressure, which could have provided interesting information about TIC variability. Additionally, the group of malignant neoplasia included only UCC; therefore, TICs might vary with other types of tumors.

In conclusion, the results of this pilot study suggest that neoplastic and non-neoplastic diseases may present different TICs. A FT higher than 10.49 s may be the only reliable cut-off to help characterizing neoplastic and non-neoplastic lesions of the urinary bladder in dogs, although this result must be interpreted with caution. A combination of laboratory findings, standard B-mode ultrasound and qualitative and quantitative CEUS analysis is still needed for further evaluation along with cytopathological confirmation. However, the results of this study need to be tested and statistically analyzed on a larger

sample since the proposed cut-off provides only limited information on the nature of UB lesions on CEUS.

Neoplastic Lesion (n = 7)					
	SI (a.u)	RT-s	mTT-s	TTP-s	FT-s
Mean	431.4	7.2	86.7	9.6	10.7
SD	781.7	6.4	114.4	7.3	4.3
Median	144.5	4.9	34.1	7.3	10.1
P25	21.4	3.6	25.4	4.8	8.9
P75	332.0	9.8	88.5	15.7	11.9
Non-neoplastic Lesion (n = 7)					
	SI (a.u.)	RT-s	mTT-s	TTP-s	FT-s
Mean	118.8267	9.023333	65.48333	12.41667	22.245
SD	126.1924	5.908227	55.48983	7.449429	18.47987
Median	79.9	8.225	44.925	12.5	16.635
P25	19.09	4.9	24.49	7.08	10.49
P75	174.39	14.1	89.64	20.18	31.62

Table 1: Statistical descriptive analysis of each contrast enhanced ultrasonographic parameter for neoplastic and non-neoplastic urinary bladder conditions in 14 dogs.

	Best cut-off	Sensitivity	Specificity	Classified	AUC
SI-a.u.	≥ 53.85 s	16.67 %	85.71%	53.85%	0.333
RT-s	≥ 6.75	66.67 %	71.43%	62.23%	0.595
mTT-s	≥ 40.83	66.67 %	57.14%	61.54%	0.523
TTP-s	≥ 9.94	66.67 %	71.43%	69.23%	0.595
FT-s	≥ 10.49	83.33 %	66.67%	75.00%	0.750

	Best cut-off	Sensitivity	Specificity	Classified	AUC
PE-r	≥ 53.85 s	16.67%	85.71%	53.85%	0.333
RT-s	≥ 6.75	66.67%	71.43%	62.23%	0.595
mTT-s	≥ 40.83	66.67%	57.14%	61.54%	0.523
TTP-s	≥ 9.94	66.67%	71.43%	69.23%	0.595
FT-s	≥ 10.49	83.33%	66.67%	75.00%	0.750
RT-s+CAT	≥ 18.9	66.67%	71.43%	69.23%	0.642
mTT-s+CAT	≥ 45.63	66.67%	57.14%	61.54%	0.547
TTP-s+CAT	≥ 25.2	66.67%	71.43%	69.23%	0.619
FT-s+CAT	≥ 29.5	66.67%	83.33%	75 %	0.722

Table 2: Summary results of receiver operating curve analyses for each contrast enhanced ultrasonographic parameter in 14 dogs with neoplastic and non-neoplastic urinary bladder disease.

Size	Mean CAT	SD	Median	P25	P75
Large (n=2)	17.3	13.8	17.3	7.5	27.1
Medium (n=9)	10.2	8.5	8.05	5.05	11.8
Small (n=3)	8	6.4	4.8	3.8	15.4

Table 3: Statistical descriptive analysis of CAT for each dog size group

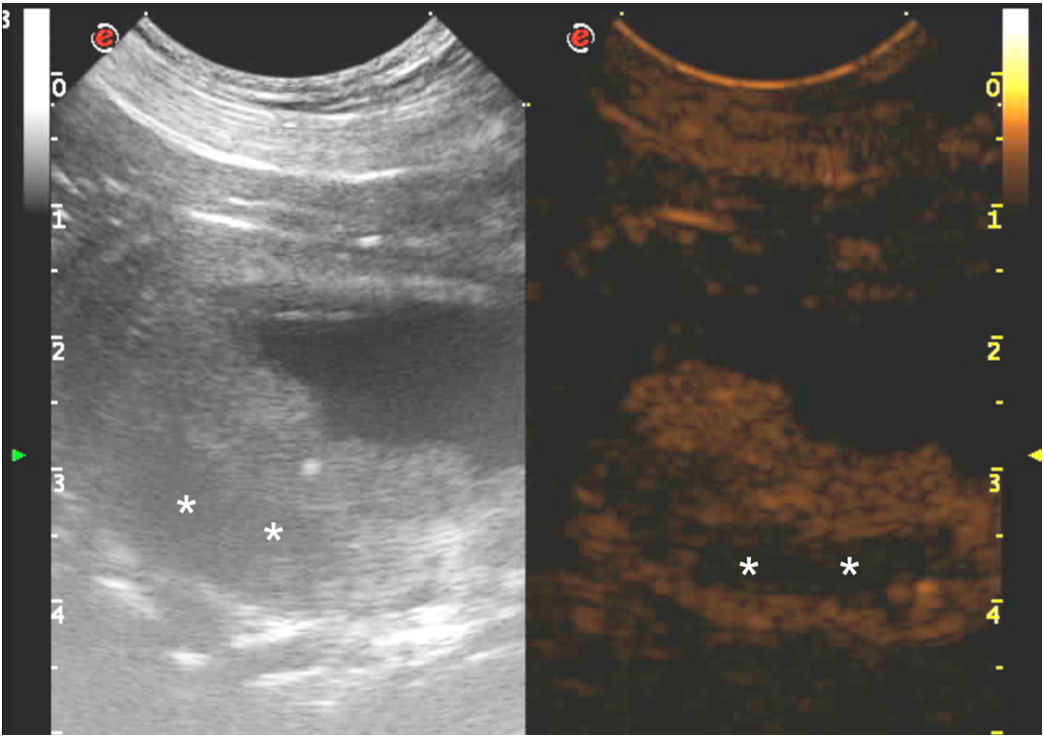

Fig. 1: Contrast-enhanced ultrasound images obtained with a multi-frequency (10-19 MHz) microconvex electronic array probe with a mechanical index of 0.3 from a dog with a neoplastic urinary bladder lesion. A: Long axis standard B-mode sonogram of the urinary bladder showing a large inhomogeneous and poorly marginated mass occupying most of the lumen with multifocal hypoechoic areas (*). B: Long axis contrast-enhanced ultrasound (CEUS) sonogram of the urinary bladder of the same lesion showing marked and heterogeneous enhancement.

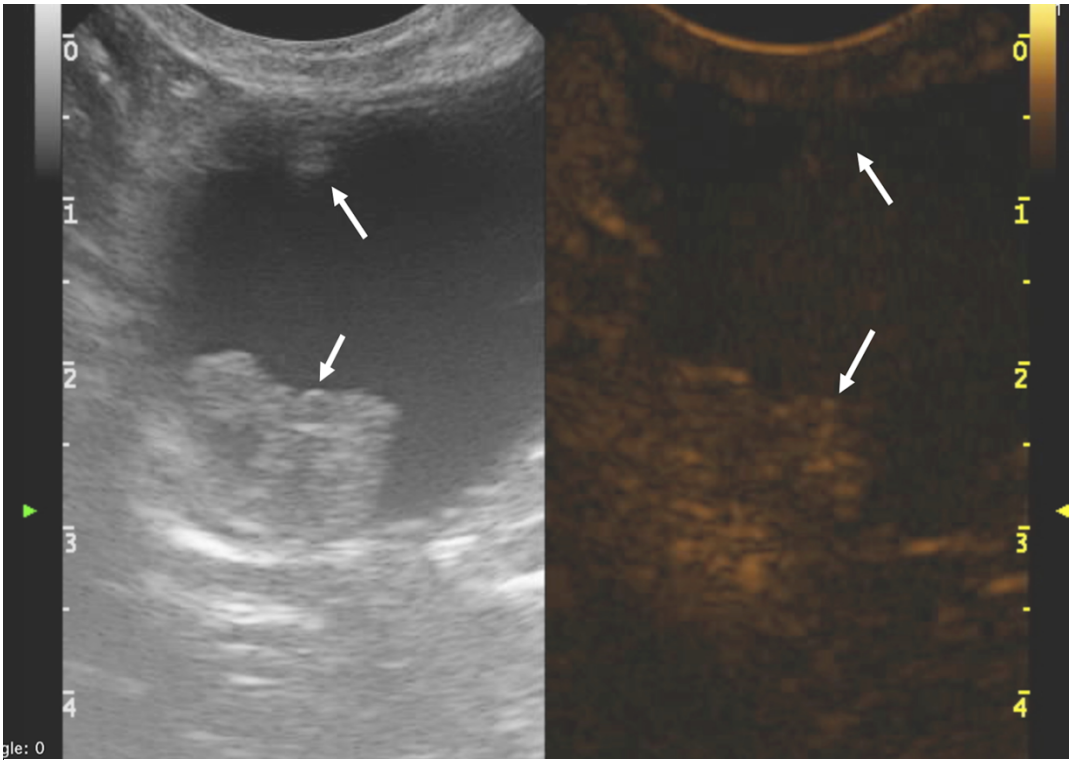

Fig. 2 Contrast enhanced ultrasound images obtained with a multi-frequency (10-19 MHz) microconvex electronic array probe with a mechanical index of 0.3 from a dog with a non-neoplastic urinary bladder lesion. A: Long-axis standard B-mode sonogram of urinary bladder showing two pedunculated lesions (arrows) extending into the bladder lumen, confirmed to be polypoid cystitis. B: Long-axis contrast-enhanced ultrasound (CEUS) sonogram of the urinary bladder of the same lesion showing moderate and homogenous enhancement.

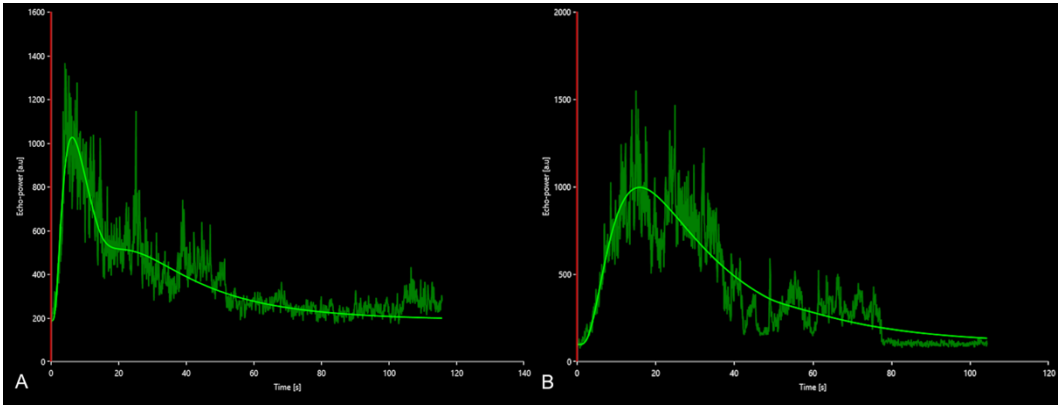

Fig. 3: Quantitative CEUS analyses performed with VueBox. TIC is created from the ROI positioned in the lesions of two representative dogs, with a neoplastic-lesion (A) and a non-neoplastic lesion (B). Neoplastic lesion (A) shows a subjectively shorter TTP and RT, higher SI, and a more rapid FT compared with non-neoplastic disease (B).

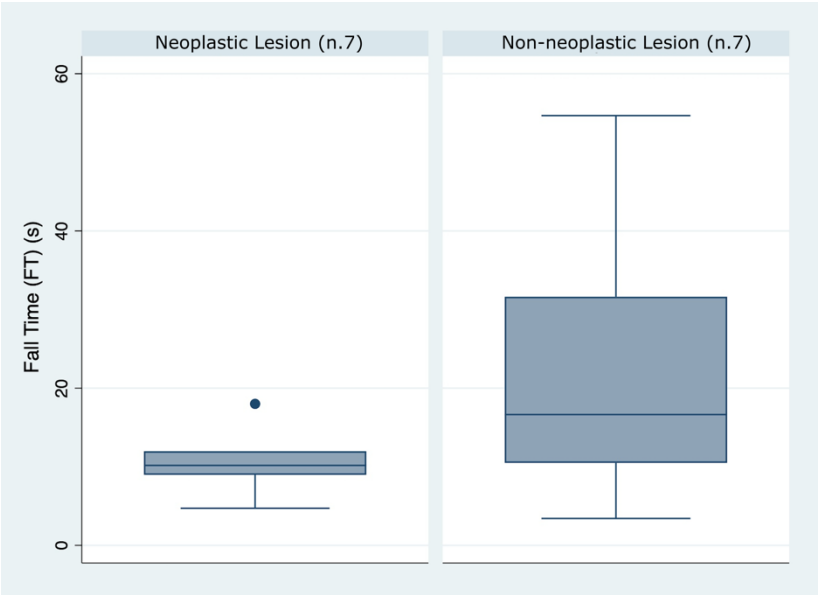

Fig. 4: Box plot showing the distribution of Fall Time values in patients belonging to the neoplastic (n=7) and non-neoplastic (n=7) group

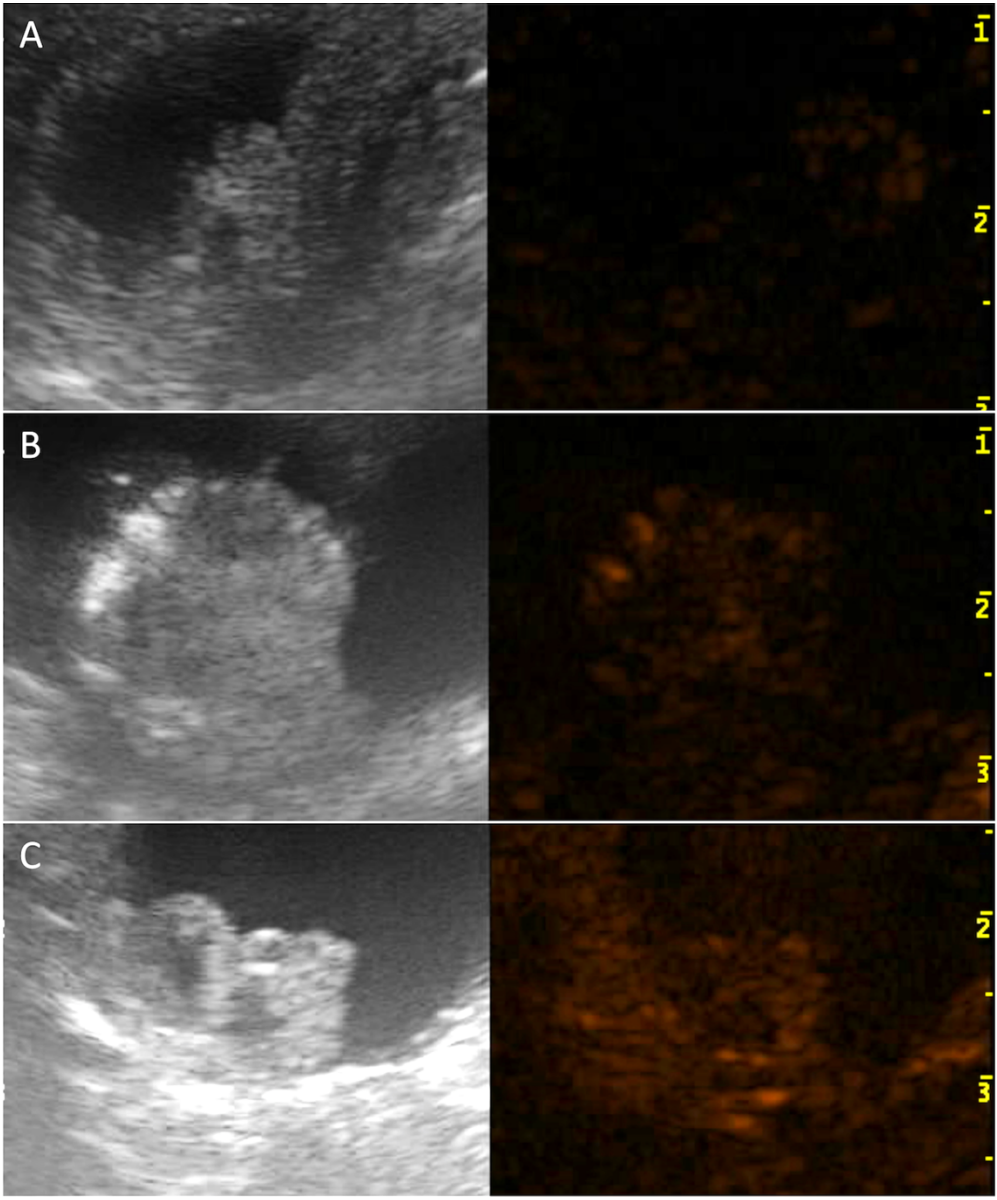

Fig. 5: Contrast-enhanced US images obtained with a multi-frequency (10-19 MHz) micro convex electronic array probes with a mechanical index of 0.3 after the injection of Sonovue. Images display three different urinary bladder lesion at the peak of contrast enhancement showing mild homogeneous enhancement (A), moderate heterogeneous enhancement (B), marked heterogeneous enhancement (C). Final diagnosis revealed inflammatory cystitis (A), urothelial cell carcinoma (B, C).

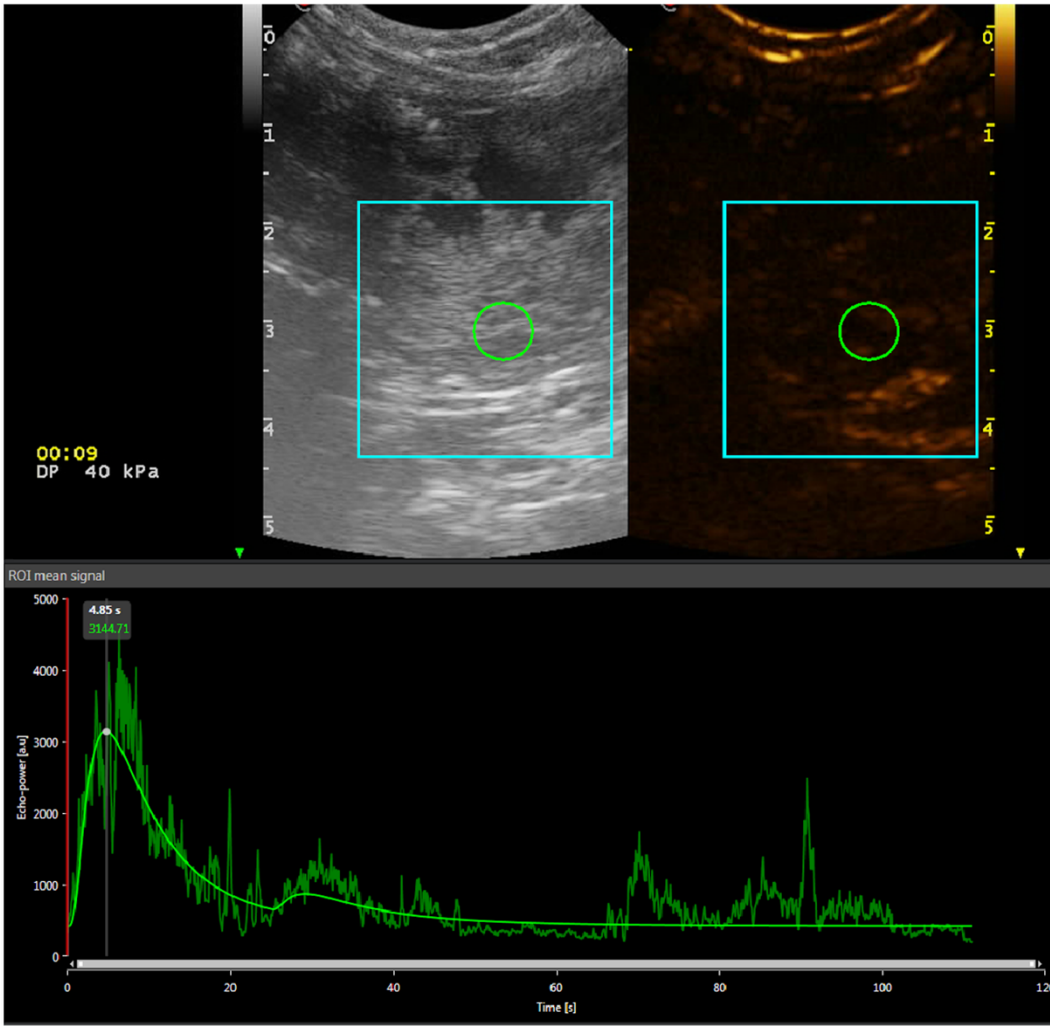

Fig. 6: Placement of the region of interest (ROI) within the parenchyma of an urothelial cell carcinoma for quantitative analysis of the mass enhancement using Vue Box commercial software. The ROI is placed within the mass, maintaining distance from areas of necrosis and lesion margins to avoid including peripheral tissues within the ROI. A time intensity curve is generated from the ROI.

References

1. Osborne CA, Low DG, Perman V, et al. Neoplasms of the canine and feline urinary bladder: incidence, etiologic factors, occurrence and pathologic features. Am J Vet Res 1968; 29: 2041–2055.
2. Nicolau C, Bunesch L, Sebastia C, et al. Diagnosis of bladder cancer: contrast-enhanced ultrasound. Abdom Imaging 2010; 35: 494–503.
3. Esplin DG. Urinary bladder fibromas in dogs: 51 cases (1981–1985). J Am Vet Med Assoc 1987; 190: 440–444.
4. Liptak JM, Dernell WS, Withrow SJ. Haemangiosarcoma of the urinary bladder in a dog. Aust Vet J 2004; 82: 215–217.
5. Mutsaers AJ, Widmer WR, Knapp DW. Canine transitional cell carcinoma. J Vet Intern Med 2003; 17: 136–144.
6. Kundu P, Ghosh D. Ultrasonographic study of urinary bladder diseases in dogs. Indian J Vet Surg 2006; 27: 33–34.
7. Petite A, Busoni V, Heinen MP, Billen F, Snaps F. Radiographic and ultrasonographic findings of emphysematous cystitis in four nondiabetic female dogs. Vet Radiol Ultrasound 2006; 47: 90–93.
8. Robotti G, Lanfranchi D. Urinary tract diseases in dogs: US findings. A mini pictorial assays. J Ultrasound 2013*;* 16: 93–96.
9. Biller DS, Partington BP, Miyabayashi T Sonographic investigation of transitional cell carcinoma of the urinary bladder in small animals. Le´Veile´R. Vet Radiol Ultrasound 1992; 33: 103–107.
10. Dinesh D, Behl SM, Singh P, Tayal R, Pal M, Chandolia RK. Diagnosis of urinary bladder diseases in dogs by using two-dimensional and three-dimensional ultrasonography. Vet World 2015; EISSN: 2231-0916; 8: 819–822.
11. Hamlin AN, Chadwick LE, Fox-Alvarez SA, Hostnik ET. Ultrasound characteristics of feline urinary bladder transitional cell carcinoma are similar to canine urinary bladder transitional cell carcinoma. Vet Radiol Ultrasound 2019; 60: 552–559.
12. Hanazono K, Fukumoto S, Endo Y, Ueno H, Kadosawa T, Uchide T. Ultrasonographic findings related to prognosis in canine transitional cell carcinoma. Vet Radiol Ultrasound 2014; 55: 79–84.
13. Jennifear H, Amy S, Tidwell D. Ultrasonographic appearance of urethral transitional cell carcinoma in ten dogs. *VeterinuryRadiology & Ultrasound;* 1996: 293–292 99.
14. Wilson HM, Chun R, Larson SV, Kurzman ID, Vail DM. Clinical signs, treatments, and outcome in cats with transitional cell carcinoma of

urinary bladder: 20 cases (1990–2004). J Am Vet Med Assoc 2007; 231: 101–106.
15. Nyland TG, Wallack ST, Wisner ER. Needle-tract implantation following US-guided fine-needle aspiration biopsy of transitional cell carcinoma of the bladder, urethra, and prostate. Vet Radiol Ultrasound 2002; 43: 50–53.
16. Takiguchi M, Inaba M. Diagnostic ultrasound of polypoid cystitis in dogs. J Vet Med Sci 2005; 67: 57–61.
17. Fulkerson CM, Knapp DW. Management of transitional cell carcinoma of the urinary bladder in dogs: a review. Vet J 2015; 205: 217–225.
18. Anderson WI, Dunham BM, King JM, Scott DWPresumptive subcutaneous surgical transplantation of a urinary bladder transitional cell carcinoma in a dog. Cornell Vet 1989; 79: 263–266.
19. Drudi FM, Cantisani V, Liberatore M, Iori F, Erturk SM, Cristini C, Di Pierro G, D'Ambrosio U, Malpassini F, De Felice C, Di Leo N. Role of low-mechanical index CEUS in the differentiation between low and hign grade bladder carcinoma: a pilot study. Ultraschall Med 2010; 31: 589–595.
20. Francisca G, Adamo Bellini S, Scarano F, et al. Correlation of transabdominal sonographic and cystoscopic findings in the diagnosis of focal abnormalities of the urinary bladder wall. A prospective study. JUM 2008; 27: 887–894.
21. Li QY, Tang J, He EH, Li YM, Zhou Y, Zhang X, Chen G. Clinical utility of three-dimensional contrast-enhanced ultrasound in the differentiation between noninvasive and invasive neoplasms of urinary bladder. Eur J Radiol 2012; 81: 2936–2942.
22. Nicolau C, Bunesch L, Peri L, Salvador R, Corral JM, Mallofre C, Sebastia C. Accuracy of contrast-enhanced ultrasound in the detection of bladder cancer. Br J Radiol 2011; 84: 1091–1099.
23. Piscaglia F, Nolsee C, Dietrich F, Cosgrove D, Gija OH, Bachmann M, Albrecht T, Barozzi L, Berlotto M, et al. The EFSUMB guid-lines and recommendations on the clinical practice of contrast enhanced ultrasound (CEUS): update 2011 on non-hepatic applications. Ultraschall Med 2012; 33: 33–59.
24. Klibanov AL, Rasche PT, Hughes MS, et al. Detection of individual microbubbles of an ultrasound contrast agent: fundamental and pulse inversion imaging. Acad Radiol 2002; 9(suppl 2): S279–S281.
25. Quaia, E. Classification and safety of microbubble-based contrast agents. In: Quaia, E., (Ed.), Contrast Media in Ultrasonography. Basic Principles and Clinical Applications 2005; Springer: Germany; pp. 3–14.

26. Seiler GS, Brown JC, Reetz JA, Taeymans O, Bucknoff M, Rossi F, Ohlerth S, et al. Safety of contrast-enhanced ultrasonography in dogs and cats: 488 cases (2002–2011). J Am Vet Med Assoc 2013; 242: 1255–1259.
27. Fus ŁP, Górnicka B. Role of angiogenesis in urothelial bladder carcinoma. Cent European J Urol. 2016;69(3):258-263.
28. Tang MX, Mulvana H, Gauthier T, et al. Quantitative contrast-enhanced ultrasound imaging: a review of sources of variability. *Interface Focus*. 2011;1(4):520-539.
29. Caruso G, Salvaggio G, Campisi A, et al. Bladder tumor staging: comparison of contrast-enhanced and Gray-Scale Ultrasound. American Journal of Roentgenology 2010; 194: 151–156.
30. Macrì F, Di Pietro S, Mangano C, Pugliese M, Mazzullo G, Iannelli NM, Angileri V, Morabito S, De Majo M. Quantitative evaluation of canine urinary bladder transitional cell carcinoma using contrast-enhanced ultrasonography. BMC Vet Res 2018; 14: 84.
31. Norris AM, Laing EJ, Valli VEO, et al. Canine bladder and urethral tumors: a retrospective study of 115 cases (1980–1985). J Vet Intern Med 1992; 6: 145–153.
32. Pollard RE, Watson KD, Hu X, Ingham E, Ferrara KW. Feasibility of quantitative contrast ultrasound imaging of bladder tumors in dogs. Can Vet J 2017; 58: 70–72.
33. Hanley JA, McNeil BJ. The meaning and use of the area under a receiver operating characteristic (ROC) curve. Radiology. 1982 Apr;143(1):29-36.
34. Knapp DW, 1995. Medical therapy of canine transitional cell carcinoma of the urinary bladder. In: Bonagura, J.D., ed. Kirk's Current Veterinary Therapy XII; W B Saunders: Philadelphia, PA; pp. 1016–1018.
35. Bryan JN, Keeler MR, Henry CJ, Bryan ME, Hahn AW, Caldwell CW. A population study of neutering status as a risk factor for canine prostate cancer. Prostate 2007; 67: 1174–1181.
36. Raghavan M, Knapp DW, Dawson MH, Bonney PL, Glickman LT. Topical flea and tick pesticides and the risk of transitional cell carcinoma of the urinary bladder in Scottish Terriers. J Am Vet Med Assoc 2004; 225: 389–394.
37. Childress MO, Adams LG, Ramos-Vara JA, Freeman LJ, He S, Constable PD, Knapp DW. Results of biopsy via transurethral cystoscopy and cystotomy for diagnosis of transitional cell carcinoma of the urinary bladder and urethra in dogs: 92 cases (2003–2008). J Am Vet Med Assoc 2011; 239: 350–356.

38. Knapp D, McMillan S, 2013. Tumors of the urinary system. In: Withrow, S.J., Page, R.L., Eds. Withrow & MacEwen's Small Animal Clinical Oncology, 5th ed.; Elsevier: St. Louis, MO, USA; pp. 572–582.
39. Inoue K, Kamada M, Slaton JW, Fukata S, Yoshikawa C, Tamboli P, Dinney CP, Shuin T. The prognostic value of angiogenesis and metastasis-related genes for progression of transitional cell carcinoma of the renal pelvis and ureter. Clin Cancer Res. 2002 Jun;8(6):1863-70.
40. Mohammed SI, Bennett PF, Craig BA, Glickman NW, Mutsaers AJ, Snyder PW, Widmer WR, DeGortari AE, Bonney PL, Knapp DW. Effects of the cyclooxygenase inhibitor, piroxicam, on tumor response, apoptosis, and angiogenesis in a canine model of human invasive urinary bladder cancer. Cancer Res. 2002 Jan 15;62(2):356-8.

3.2. Paper two: Computed tomographic appearance of transcaval ureter in two dogs and three cats: a novel CVC congenital malformation

C. Spediacci [1,] M. Longo[1;7-8], S. Specchi [2], P. Pey [3;8], S. Rabba [4], E. Mavraki [6], M. Di Giancamillo [1], I. Panopoulos [5]

[1] Department of Veterinary Medicine and animal science (DIVAS), University of Milan, Street of University n. 6, 26900, Lodi (LO), Italy
[2] Ospedale Veterinario i Portoni Rossi,Via Roma 57, Zola Predosa, Bologna 40069, Italy.
[3] Service d'Imagerie Médicale, Centre Hospitalier Universitaire Vétérinaire d'Alfort, Ecole Nationale Vétérinaire d'Alfort, Maisons-alfort 94007, France. Dr. Pey is now working for Antech Imaging services, Irvyne, California and OspedaleVeterinario i Portoni Rossi,Via Roma 57, Zola Predosa, Bologna 40069, Italy.
[4] Department of Diagnostic Imaging, Istituto Veterinario di Novara, Granozzo con Monticello (NO), Italy
[5]Alphavet veterinary diagnostic imaging centre, Kifisia, Athens, Greece
[6]Vets4life veterinary clinic, Pikermi, Athens, Greece
[7]C.T.O. Veterinario, via C.Festa 9 Arenzano (Genova), 16011, Italy
[8]Antech Imaging Services, Irvine, CA , United States

Corresponding author: Carlotta Spediacci
(carlotta.spediacci@unimi.it)

Key words: peri-ureteral venous ring, caudal vena cava malformation, canine, feline, imaging

List of abbreviation
CVC: caudal vena cava; IVC: inferior vena cava; CT: computed tomography; HU: Hounsfield unit; PACS: Picture Archiving and Communication System; MDTC: Multidetector Computed Tomography

Abstract

Transcaval ureter is a rarely reported human congenital malformation of the pre-renal segment of the inferior vena cava (IVC) not yet reported in veterinary medicine. The objective of this multicenter retrospective case series study was to describe the computed tomography (CT) features of transcaval ureters in dogs and cats.

Patients referred for pre- and post-contrast CT exam of the abdomen and presenting this abnormality were retrospectively included.

Multiple qualitative features were described for each ureteral abnormality detected. Three cats and two dogs with caudal vena cava (CVC) malformation were identified consisting in a segmental duplication of the CVC at the pre-renal level creating a vascular ring through which the ureter extended, identified as a *double-barrel gun* sign. The malformation was divided in two types according to the symmetry of the caval branches and

location in relation with the aorta: type I symmetrical branches and right-lateral to aorta, type II asymmetrically branches and right-dorsal to aorta.

In one case the malformation was associated with hydroureter and mild pyelectasia. In three cases, the anomaly was incidental and in the remaining two cases the clinical significance was uncertain.

This is the first study describing the presence of transcaval ureter in dogs and cats. Computed tomography was a suitable method for the diagnosis of transcaval and a focal *double-barrel gun* sign of the CVC is proposed as the hallmark feature of this anomaly. The clinical relevance of this congenital vascular malformation is unclear and needs to be further investigated.

Introduction

Variation in the anatomy of caudal vena cava (CVC) may have important clinical implication. In-depth knowledge of its

anatomy is fundamental to prevent any potential medical and surgical complication related to anatomical variation of the CVC.[1-4]

Normal embryogenesis of the CVC leads to the origin of a single vessel positioned to the right of the aorta artery.[4,5] It is created by persistence, regression, and anastomosis of three bilateral symmetrical embryonic veins: the postcardinal, the subcardinal and supracardinal. An anomaly in the development of these vessels results in congenital vascular anomalies of the CVC. [4-7]

In veterinary medicine, several well recognized congenital anomalies of the CVC have been reported, including double CVC and retrocaval ureter.

Contrast enhanced multidetector computed tomography (MDCT) for detecting and characterize CVC anomaly is recommended due to the excellent visualization of the CVC and its relationship with the ureters. [5]

Transcaval ureter is a rare embryological abnormality of the inferior vena cava (IVC) rarely described in human medicine, in which a segmental duplication of this vessel creates a venous ring that encircles the right ureter. [14-17] There are few reports on transcaval ureter in human medicine and different theories about its embryological development were formulated.[2;14-17] According to the supracardinal model, transcaval ureter arises when the right posterior cardinal and right supracardinal veins fail to regress in post-renal segment, resulting in a partial duplication of IVC that creates a venous ring thorough which the right ureter extends. The reported prevalence of transcaval ureter in human is about 0.9 in 1000 with a male-to-female ratio of 2.8:1. [18] This abnormality in human patients is described as often asymptomatic, but can sometimes result in flank pain, hydro-ureteronephrosis, recurrent urinary infections, increased frequency of urination and haematuria. [19-21]

To the authors' knowledge, this anomaly and the computed tomography (CT) features of the transcaval ureter have never been reported in veterinary medicine. The aim of the authors was to describe the computed tomographic characteristics of transcaval ureters in case series dogs and cats.

Material and Method

This was a retrospective, descriptive, multi-center, case series design study.

Clinical cases from different Institutions (I Portoni Rossi, University Veterinary Hospital d'Alfort, Istituto Veterinario di Novara, C.T.O. Veterinario and Alphavet Clinic) were searched for dogs and cats with a diagnosis including the keywords "atypical CVC malformation". Permission to use clinical and diagnostic imaging data for research was provided through informed consent from the owners at the time of admission. Criteria for inclusion in the study were a final diagnosis of

unclassified vascular malformation consisted in a venous ring encircling the ureter and originating from the CVC and an available CT study of diagnostic quality of the abdomen before and after intravenous contrast medium injection. Patients were included regardless of sex, breed, age, clinical signs and acquisition parameters or scanner types (16 and 64 slices). Decision for study inclusion were based on a common consensus between all authors.

Medical records were reviewed regarding species, age, breed, sex, body weight, clinical signs and final diagnosis. Pre- and post-contrast images were stored on a dedicated PACS and evaluated by four ECVDI (PP, IP, ML, SR) and one ACVR (SS) -board certified veterinary specialists. All assessments were performed using a dedicated DICOM viewer software (OsiriX Imaging Software, v 3.9.2., Pixmeo, Geneva, Switzerland). A soft tissue window width of 350 Hounsfield Unit (HU) and a window level of 50 HU were used. In all cases the images were

reconstructed in multiple reformatted planes and on 3D, if needed. The segmental bifurcation of the CVC in cross-section assumed the appearance of two adjacent round structures that have been defined as '*double-barrel gun sign*'. The following parameters of the CT scan were recorded: position of the venous ring in relation to aorta and lumbar spine, diameter of the ureter proximal and distal to the venous ring expressed in millimeters, presence of pyelectasis, thrombosis, concomitant congenital malformation. Ureteral dilation if present was diagnosed when the maximal diameter of the cross-section of the ureter was measuring more than 2.5 mm in dogs and cats. [22-23] Pyelectasis was diagnosed when the maximal diameter of the renal pelvis was measuring more than 3 mm in both dogs and 3 mm cats. Renal pelvis > 6 mm was defined as suggestive of suspected mechanical obstruction while > 13 mm was defined as unequivocally obstructed. [24-26]

All assessments were based on visual inspection. Computed tomographic images were assessed blindly, without knowledge of the signalment and clinical findings from the patients. If there were different opinions about CT findings, a final diagnosis was made based on consensus of all the observers. Additional unrelated CT findings were recorded, when observed.

Results

Case 1

An eleven-year-old intact female domestic shorthaired cat was presented to Instituto Veterinario Novara for a whole-body pre and post-contrast CT exam for staging of mammary nodules.

No clinical signs referable to anomalies of the urinary tract were reported. Blood biochemistry and urinalysis were normal. Urine culture was not available. Computed tomography revealed a unilateral transcaval ureter, in which the right ureter emerged through a venous ring formed by a segmental duplication of the

CVC at the level of L4-L5. The two branches of the CVC were symmetrical in diameter with a *double-barrel gun* appearance and normally located right-ventral to the aorta. The diameter of the ureter both proximal and distal to the venous ring measured normal 0.6 mm. [23] Other CT findings were mammary nodules associated with inguinal lymphadenopathy and bilateral renal infarcts. There was no evidence of thrombosis, pyelectasis, ureteral dilation or other concomitant congenital malformation.

Case 2

A four-year-old Maltese neutered male dog was referred to Alphavet Diagnostic Imaging center for an abdominal pre and post-contrast CT exam and a 4-month history of recurrent vomiting. The patient did not show improvement after medical treatment consisting of metoclopramide and ranitidine performed at the referring veterinarian. Blood biochemistry showed renal enzymes within normal ranges, while biliary acids were slightly increased at 4.9 micro mol/L (normal range 0.2 to

4.3 micro mol/L). Urine culture was not available. The referring veterinarian suspected chronic hepatitis. Computed tomography revealed a unilateral transcaval ureter, in which the right ureter emerged through a venous ring at the level of L3-L4. The two branches of the CVC were symmetrical in diameter with a *double-barrel gun* appearance and normally located right-ventral to the aorta. The ureter proximal to the venous ring was homogeneously distended (diameter 9.6 mm) with associated mild pyelectasis (3.4 mm).[24-26] Distal to the venous ring the ureter measured normal (1.4 mm).[13] There was no evidence of thrombosis, or other concomitant congenital malformation.

Case 3

A six-year-old medium-size mixbreed neutered female dog was presented to the C.T.O. Veterinario for abdominal pre and post-contrast CT exam to investigate causes of hematuria. Blood biochemistry and urine culture were normal. On urinalysis the specific gravity (USG) was 1.100, pH 6, blood 1+. Urine

sediment revealed mild presence of red blood cells. On CT examination a right transcaval ureter was found. Computed tomography revealed a unilateral transcaval ureter, in which the right ureter emerged through a venous ring at the level of L3-L4. The two branches of the CVC were symmetrical in diameter with a horizontal *double-barrel gun* appearance and normally located right ventral to the aorta. Proximal and distal to the venous ring the right ureter measured normal (1.7 mm).[22] There was no evidence of thrombosis, pyelectasis, ureteral dilation or other concomitant congenital malformation.

Case 4

A two-year-old domestic shorthaired neutered female cat was presented to the Centre Hospitalier Universitaire Vétérinaire d'Alfort for a whole-body pre and post-contrast CT exam. The patient had a history of a car accident 24-hour before presentation. Patient presented with pelvic fractures and absence of deep pain on the hindlimbs. No clinical signs referable to

anomalies of the urinary tract were reported. Blood biochemestry and urinalysis were normal. Urine culture was not performed. Computed tomography revealed a unilateral transcaval ureter, in which the right ureter emerged through a venous ring at the level of L4-L5. The two branches of the CVC were symmetrical in diameter with a *double-barrel gun* appearance and located lateral the aorta. The diameter of the right ureter proximal and distal to the venous ring was slightly increased (0.4 mm).[23] Other CT findings consisted in comminuted and displaced non-articular closed traumatic fractures of the pubis and right ileus with concomitant left sacroiliac luxation. There was no evidence of thrombosis, pyelectasis, or other concomitant congenital malformation.

Case 5

A pre and post-contrast CT exam of the thorax, abdomen and spine of a 5-year-old domestic shorthaired neutered female cat was submitted as a teleradiology consult to Antech Imaging

Services. The referred clinical signs of the patient consistent in acute onset of pelvic limb ataxia. Blood biochemestry and urinalysis were normal. Urine culture was not performed. Computed tomography findings consisted with the presence of a pulmonary mass, while the spine appeared unremarkable. In the abdomen, a unilateral transcaval ureter, in which the right ureter emerged through a venous ring extending from L3 to L6 was detected. The two branches of the duplicated CVC were asymmetrical with a *double-barrel gun* appearance, in which the dorsal branch had a smaller diameter, and it was positioned right dorsal to the aorta. Diameter of the right ureter both proximal and distal to the venous ring was normal (0.3 mm).[23] There was no evidence of thrombosis, left hydronephrosis, ureteral dilation or other concomitant congenital malformation.

In this patient, duplication of the spleen was also detected. Other findings consisted in left psoas muscles changes and jejunal lymphadenopathy. No evidence of thrombosis and pyelectasis.

Discussion

To the authors knowledge this is the first case series describing the presence and the CT appearance of transcaval ureter in dogs and cats. In all cases described in this study the transcaval ureter was unilateral to the right and appeared as a vascular ring of the CVC through which the right ureter passed identified as *double barrel-gun sign*. In only one case hydronephrosis and mild pyelectasis were associated.

The CVC is composed of four major segments: prerenal, renal, prehepatic and posthepatic. The prerenal segment forms from the confluence of the common iliac veins to the right of the aortic trifurcation, along with the confluence of the right gonadal vein. The renal segment forms ventrally and to the right of the abdominal aorta, from the union of the right and left renal veins with the left gonadal vein. Finally, the prehepatic, hepatic and posthepatic course to the right dorsal portion of the liver. [7-9] Various hypotheses have been formulated to explain the origins

of the prerenal segment of the CVC. The most accepted theory is the 'supracardinal model'. This theory assumes that the retroperitoneal venous system is developed from three paired fetal veins: the posterior cardinal, the supracardinal and the subcardinal veins. During embryological development of the CVC, the left supracardinal vein and the lumbar portion of the right posterior cardinal vein normally regress. The subcardinal vein becomes the internal spermatic vein and the right supracardinal vein develops into the definitive right CVC. [9-11]

In accordance with the human literature, all dogs and cats included in this study reported a right-sided distribution of the transcaval ureter. [14-17] Only patient number 3 had limited clinical signs related to the urinary system, consistent with hematuria which is also reported in human medicine.[14-15] All the patients included in this case series displayed normal kidney values. This is also similar to what reported in people, as kidney function is

unchanged despite possible gross changes of the ureter.[2] For example, in cases of ureteral ectopia, the normal renal function is possibly related to the congenital origin of the anomaly and the adaptive process of the urinary tract during the development.[33]

Patient number 2 had intermittent vomiting despite absent gastrointestinal changes on CT. Flank pain might be considered in the differentials as a possible reason for the clinical signs, triggered by colic irradiation due to ureteral stretch, as reported in humans.[15] However, a significant limitation regarding this hypothesis is that no additional procedures, such as gastrointestinal endoscopy and biopsy, were performed to further investigate the cause of vomiting.

A moderate right hydroureter and mild ipsilateral pyelectasis was also detected in patient number two. This has some similar characteristics to retrocaval ureter type I ('fishhook deformity'). Nevertheless, in this type of retrocaval ureter there is an extreme

medial deviation of the middle ureteral segment where it passes behind the IVC/CVC, usually at the L3 vertebral level. [3] In our case, the deviated portion of the ureter splits the CVC and therefore courses gently medially rather than in a typical type I retrocaval ureter. In addition, the level of mechanical obstruction due to the vascular ring was located more caudally compared to a typical retrocaval ureter. Although the pelvic dilation was mild, guidelines of American College of Veterinary Internal Medicine (ACVIM) indicate that hydronephrosis and hydroureter proximal to an obstructive lesion are sufficient to diagnose mechanical obstruction. [23] Therefore, in this patient ureteral obstruction is likely caused by the vascular malformation. However, due to the absence of clinical signs and normal renal parameters, further treatment and investigations were discarded. Hydroureter and pyelectasis may predispose to recurrent urinary tract infection. In human medicine surgical management is recommended in case of complications,

including recurrent urinary infections, urolithiasis or impaired renal function. [27]

In patient one renal infarcts were found on the CT examination. In humans, anomalies of the IVC have been reported to be a risk factor for development of deep vein thrombosis. However, this has not been described in veterinary medicine, therefore a correlation between renal infarcts and transcaval ureter should be considered cautiously.[35,36]

In human and veterinary medicine, congenital anomalies of the IVC/CVC are increasingly recognized in asymptomatic patients due to the increased use of cross-sectional imaging technique such as CT, offering simultaneous evaluation of the vascular system and urinary tract with the aid of uroangiographic ICM.[28] Although the anomalies of the vessels and ureters are often clinically silent, it is important recognize them in order to avoid potential complication during surgery and interventional

radiology procedures.[29] In humans, CT angiography provides precise preoperative information about abdominal vascular anatomy, with reported accuracy of >97% for arteries and 96-100% for veins. [29]

Transcaval ureter may show similarities with retrocaval ureter, in which the ureter run medially to the CVC, and therefore should be considered in the differential diagnosis and diagnostic process. [16]

Retrocaval ureter occurs as a result of abnormal persistence of the right cardinal vein, which is crossed dorsally and medially by the ipsilateral ureter. A prevalence of 22.4% was reported with the right kidney involved 13.3% times more frequently than the left. [5;12] Two types of retrocaval ureter are described in human medicine and the same classification has been used in veterinary medicine: type I, or low loop, and type II, or high loop.[30-32] The Type 1 is described as a possible cause of ureteral obstruction while Type 2 is associated with mild or no

hydronephrosis and occurs in only 10% of patients.[30] Transcaval ureter is not susceptible to this specific classification despite showing characteristics in between these two types.[1] A focal *double-barrel gun* sign of the CVC is proposed as the hallmark sign of the anomaly, which should be recognized and differentiated from a common retrocaval ureter. A clear and direct identification of the defect can only be achieved by a late venous post contrast CT exam, allowing simultaneous visualization of the CVC and ureter. Nevertheless, detection of the defect can be challenging and may require multiplanar or 3D multiplanar reconstructions.

In human medicine surgical management involves resection of the ureter and an ureteroureteric anastomosis anterior to the IVC.[15] To the authors knowledge, there is no surgical procedure described in veterinary medicine for treatment of a transcaval ureter since this congenital malformation has never been

described and its clinical impact is still uncertain. However, division of the dilated renal pelvis with transposition and anastomosis, ureterotomy or resection of the stenotic segment of ureter compressed by the anomalous vessel with anastomosis of a double-J stent, and ligation or transection of the CVC with or without anastomosis are also procedures indicated in case of renal obstruction. [30,34]

The association of congenital anomalies of the CVC/IVC with other malformations is reported in both human and veterinary medicine, but the incidence is still unclear because these anomalies might be often underdiagnosed. In small-breed dogs is reported that 7% of patients with malformation of CVC might present with a concomitant extrahepatic portosystemic shunt, while a left-sided circumcaval ureter was reported in association to transposition of the CVC.[5,28,35]

In the present case series, the only concomitant congenital anomaly found was duplication of the spleen in one patient, however for the authors knowledge this anomaly has never previously been associated with IVC/CVC malformations.[37] Furthermore, in this case series two vascular patterns of the transcaval ureter have been described. The first type consisted of a *double-barrel gun* appearance with symmetrical vascular branches, normally located right ventral to the aorta. The second type consisted of a *double-barrel gun* sign with asymmetrical vascular branches located right dorsal to aorta. Previous studies have reported that asymmetry of venous diameters in cases of caudal vena cava duplication is secondary to a regression disorder of the supracardinal vein, which may be located dorso-laterally to the aorta in the caudal portion of the prerenal segment.[28,35] Despite this theory was formulated for duplication of IVC/CVC, the authors speculate that similar embryogenetic

processes may also be involved in generating this particular pattern of congenital malformation.

Multidetector angiographic CT exam in all cases demonstrated to be a valid technique in the diagnosis of transcaval ureter allowing simultaneous assessment of ureters and CVC. In addition, techniques such as multiplanar and three-dimensional reconstruction, including volume rendering, can be used to further investigate the morphology of the defect. In particular, multiplanar reconstruction can assist in understanding the anatomy and the relationship between the ureter and the vascular ring.

Limitations of this study are related to the retrospective and multicentric design. Indeed, CT exam parameters and scanners were not standardized and the quality of the urographic excretory phase was not standardized either. Furthermore, there

was inconsistence of data collection and complete urianalysis and additional examinations such as cystoscopy, pyelocentesis or biopsy were not available in these series of patients. A further limitation is due to the retrospective data collection which might have affected the inclusion of additional cases.

In conclusion, transcaval ureter is a novel congenital malformation of the CVC in dogs and cats. The tomographic sign of transcaval ureter in both dogs and cats consists in a segmental duplication of the CVC at the pre-renal level, creating a vascular ring through which the ureter extends, identified as a *double-barrel gun* sign. Further studies are needed in order to determine the clinical significance of this novel congenital malformation.

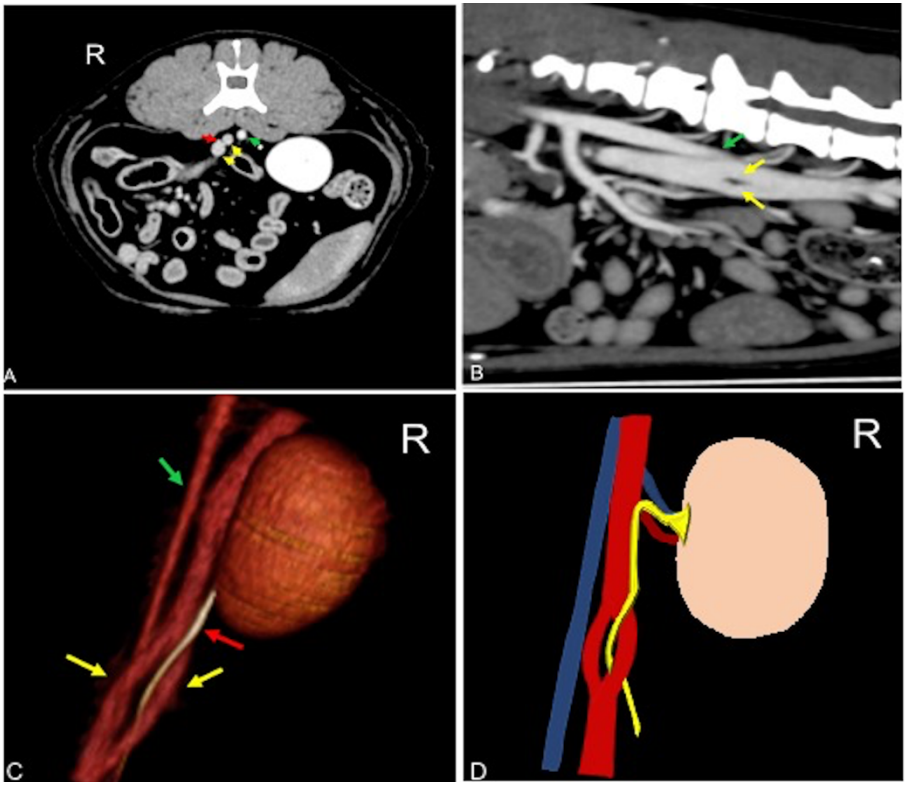

Fig. 1: Postcontrast computed tomographic of mid abdomen in transverse (A), sagittal (B), volume rendering image in a right-dorsal view (C) and schematic representation of the malformation (D) showing the CVC venous ring (yellow arrow) described as double barrel-gun sign with the right ureter (red arrow) passing through it. The venous malformation is normally located right ventral to aorta (green arrow). Soft tissue reconstruction (window level: 40 HU, window width 400 HU) and a slice thickness of 1.25 mm were used. In the image D the aorta is blue, the CVC is red, and the ureter is yellow. R: right.

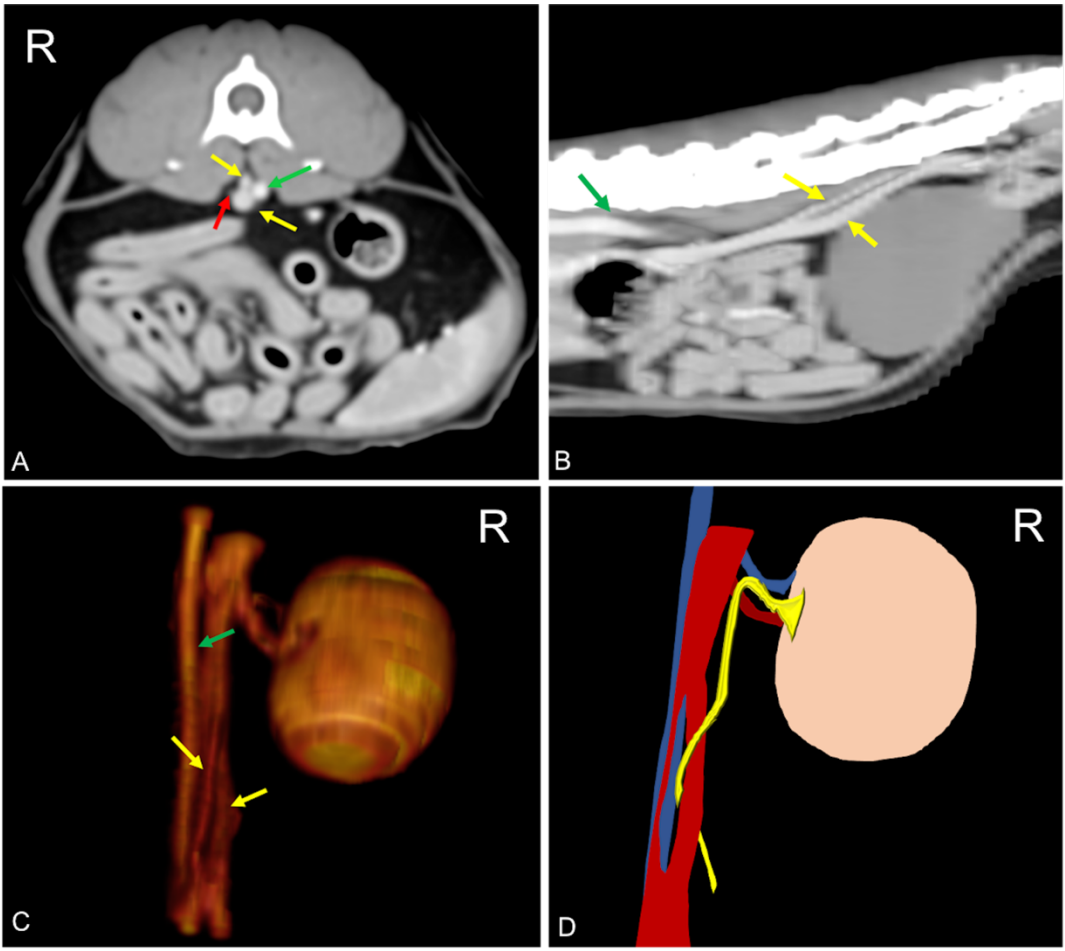

Fig. 2: Postcontrast computed tomographic of mid abdomen in transverse (A), sagittal (B), volume rendering image in a right-dorsal view (C) and schematic representation of the malformation (D) showing the CVC venous ring (yellow arrow) described as double barrel-gun sign with the right ureter (red arrow) passing through it. The two branches of the venous ring appear asymmetric with the dorsal branch located dorsally to aorta (green arrow). Soft tissue reconstruction (window level: 50 HU, window width 350 HU) and a slice thickness of 2.5 mm were used. In the image D the aorta is blue, the CVC is red, and the ureter is yellow. R: right.

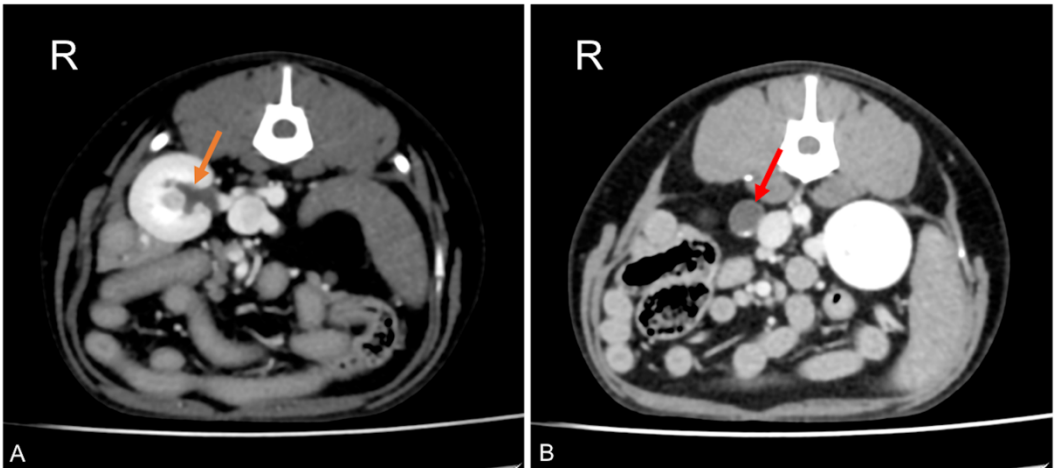

Fig. 3: Postcontrast computed tomographic images of mid abdomen in transverse views at the level of the right kidney (A) and just proximally to the venous ring (B) in a dog showing dilation of the renal pelvis (orange arrow) and dilation of the right ureter proximally to the venous ring malformation (red arrow). Soft tissue reconstruction (window level: 40 HU, window width 400 HU) and a slice thickness of 1.25 mm were used. R: right.

References

1. Bateson EM, Atkinson D. Circumcaval ureter: A new classification. Clin Radiol. 1969; 20:173-7. 9.
2. LePage JR, Baldwin GN. Obstructive periureteric venous ring. Radiology. 1972; 104:313-5.
3. Phillips E. Embryology, normal anatomy, and anomalies. In: Ferris EJ, Hipona FA, Kahn PC, Phillips E, Shapiro JH (eds) Venography of the Inferior Vena Cava and its Branches. Baltimore: Williams & Wilkins. 1969; 1-32
4. Bass JE, Redwine MD, Kramer LA, et al. Spectrum of congenital anomalies of the inferior vena cava: cross-sectional imaging findings. Radiographics. 2000; 20:639–52.
5. Pey, P., Marcon, O., Drigo, M., Specchi, S. and Bertolini, G. Multidetector-row computed tomographic characteristics of presumed preureteral vena cava in cats. Vet Radiol Ultrasound. 2015;56: 359-366.
6. McClure CFW, Butler EG. The development of the vena cava inferior in man. Amer J Anat. 1925; 35:331–83.
7. Kandpal H, Sharma R, Gamangatti S, Srivastava DN, Vashisht S. Imaging the inferior vena cava: A road less traveled. Radiographics. 2008; 28:669-689.
8. Cornillie P, Simoens P. Prenatal development of the caudal vena cava in mammals: Review of the different theories with special reference to the dog. Anat Histol Embryol. 2005; 34:364-372.
9. Hunt, Bellenger, Borg, Youmans, Tisdall,Malik. Congenital interruption of the portal vein and caudal vena cava in dogs: Six case reports and a review of the literature. Vet Surgery. 1998; 27:203-215
10. Bezuidenbout AJ. Veins. In: Evans HE, de Lahunta A, eds. *Miller's Anatomy of the Dog*. St. Louis, MO Elsevier Saunders. 2013505-534.
11. Schwarz T. Systemic and portal abdominal vasculature. In: Schwarz T, Saunders J, eds. Veterinary Computed Tomography. West Sussex, UK Wiley-Blackwel. 2011:357-370.

12. Caceres, Zwingernberger, Aronson, Mai. Characterization of normal feline renal vascular anatomy dual-phase CT angiography. Veterinary Radiology & Ultrasound 2008. 49: 350-356.
13. Bertolini. CT Angiography and Vascular Anomalies. Advances in Small Animal Care. 2020; 1: 49-47.
14. Arya MC, Baid M, Tiwari R, Vasudeo V, Singh A. Transcaval ureter: A rare embryological anomaly of inferior vena cava causing obstructive uropathy. Urol Sci. 2019; 30:86-8.
15. Giddy S, Thangasamy I, Vega Vega A. Transcaval ureter: a rare embryological anomaly causing obstructive uropathy. BMJ Case Rep. 2015; bcr2014208076.
16. Totti Cavazzola L, Groisman R, Fernando de Olivera. Transcaval ureter: case report and review of the literature. Eur J Anat. 2005; 9: 59-62.
17. Sofia C, Racchiusa S, Magno C, Inferrera A, Donato R, Mucciardi G, Mazziotti S, Ascenti G. Transcaval Ureter: Multidetector Computed Tomography Demonstration. Urology. 2015; 86(1):3-4.
18. N. T. Johansson, Sv. Nilsson, T. Scherstén, J. Schvarcz & P. O. Weiland. Retrocaval Ureter: Report of a Case and Short Review of the Literature, Scandinavian Journal of Urology and Nephrology. 1969; 3:53-58.
19. Dharman K. Transcaval ureter. J Urol. 1980 Apr;123(4):575-6.
20. Gong J, Jiang H, Liu T, Yuan Q, Sun L, Yang J, Xu J. Imaging of partial right double vena cava with ureter crossing through its split, confirmed at surgery. Clin Imaging. 2011; 35(2):148-50.
21. Gupta NP, Nayyar R, Sahay SC. Periureteric venous ring with renal calculi and transitional cell carcinoma: report of a rare case. Surg Radiol Anat. 2010; 32(4):405-7.
22. Rozear L, Tidwell AS. Evaluation of the ureter and ureterovesicular junction using helical computed tomographic excretory urography in healthy dogs. Vet Radiol Ultrasound. 2003; 44(2):155-64.
23. Testault, I, Gatel, L, Vanel, M. Comparison of nonenhanced computed tomography and ultrasonography for detection of ureteral calculi in cats: A prospective study. J Vet Intern Med. 2021; 35(5): 2241- 2248.

24. D'Anjou, Bedard, Dunn. Clinical significance of renal pelvic dilatation on ultrasound in dogs and cats. Veterinary Radiology & Ultrasound. 2011; 52: 88-94.
25. Quimby JM, Dowers K, Herndon AK, Randall EK. Renal pelvic and ureteral ultrasonographic characteristics of cats with chronic kidney disease in comparison with normal cats, and cats with pyelonephritis or ureteral obstruction. J Feline Med Surg. 2017;19(8):784-790.
26. Lemieux C, Vachon C, Beauchamp G, Dunn ME. Minimal renal pelvis dilation in cats diagnosed with benign ureteral obstruction by antegrade pyelography: a retrospective study of 82 cases (2012-2018). J Feline Med Surg. 2002; 23(10):892-899.
27. Lulich JP, Berent AC, Adams LG, Westropp JL, Bartges JW, Osborne CA. ACVIM Small Animal Consensus Recommendations on the Treatment and Prevention of Uroliths in Dogs and Cats. J Vet Intern Med. 2016;30(5):1564-1574.
28. Ryu C, Choi S, Choi H, Lee Y, Lee K. CT variants of the caudal vena cava in 121 small breed dogs. Vet Radiol Ultrasound. 2019;60(6):680-688.
29. M Pozniak, D J Balison, F T Lee, Jr, R H Tambeaux, D T Uehling, and T D Moon. CT angiography of potential renal transplant donors. RadioGraphics. 1998; 18: 565-587.
30. Salonia A, Maccagnano C, Lesma A, et al. Diagnosis and treatment of the circumcaval ureter. European urology supplements. Amsterdam: Elsevier BV. 2006;449–462.
31. Lee S, Kim W, Jeong HJ, et al. Retrocaval ureter. Kidney Int 2006; 70:615.
32. Bélanger R, Shmon CL, Gilbert PJ, Linn KA. Prevalence of circumcaval ureters and double caudal vena cava in cats. Am J Vet Res. 2014 Jan;75(1):91-5.
33. Secrest, Scott A et al. Comparison of transverse computed tomographic excretory urography images and maximum intensity projection images for diagnosing ectopic ureters in dogs. Veterinary Radiology & Ultrasound. 2017; 58: 163–168.
34. J.Steinhaus, A.C Berent, C.Weisse, A.Eatroff, T.Donovan, J.Haddad, and D.Bagley. Clinical presentation and outcome of cats with

circumcaval ureters associated with a ureteral obstruction. J Vet Intern Med. 2015; 29: 6363-70.
35. Bertolini G, Diana A, Cipone M, Drigo M, Caldin M. Multidetector row computed tomography and ultrasound characteristics of caudal vena cava duplication in dogs. Vet Radiol Ultrasound. 2014; 55(5):521-30.
36. Sarlon G, Bartoli MA, Muller C, Acid S, Bartoli JM, Cohen S, Piquet P, Magnan PE. Congenital anomalies of inferior vena cava in young patients with iliac deep venous thrombosis. Ann. Vasc. Surg. 2011;25(2): 265.
37. Battiato P, Salgüero R, Specchi S, Longo M. Ultrasonographic and CT diagnosis of a complete splenic duplication with right splenic torsion and presumed regional splenic vein hypertension in a dog. Vet Radiol Ultrasound. 2022; 63(1): 1-5.

3.3. Paper three: High field Magnetic Resonance T2 sequences are feasible to assess the ureters in healthy dogs

Carlotta Spediacci [1] DVM; Sofia Roumelioti [2] DVM; Giulia Sala [1] DVM, PhD, Ioannis Panopoulos [2] DVM PhD Dipl ECVDI; Mauro Di Giancamillo [1] DVM, Full Professor; Maurizio Longo [1] DVM PhD Dipl ECVDI

[1] Departement of Veterinary Medicine and Animal Science (DIVAS), University of Milan, Street of University n. 6, 26900, Lodi (LO), Italy
[2] Alphavet veterinary diagnostic imaging centre, Kifisia, Athens, Greece
Corresponding author: Carlotta Spediacci (carlotta.spediacci@unimi.it)

Key Words: *Canine, Ureteral, Imaging, MR, normal anatomy*

Conflict of Interest: the authors declare that there is no financial interest related to article content.

Previous Presentation Disclosure: the authors declare that this work was not previously presented.

Acknowledgments: The authors would like to thank the owners of the patients selected for this study.

Abstract

In veterinary medicine CT and US are commonly used for the evaluation of the diseases in the urinary tract, particularly at the level of the ureters. In the last decade, few studies have been performed to investigate the diagnostic capabilities of MR for the assessment of urinary tract disease, mainly focusing on the renal vascularization and function.

The aim of this retrospective design study was to describe the appearance, course and characteristics of the ureters in high-field 1,5T MR using T1, T2 and T2 fat-sat weighted sequences without the use of gadolinium contrast agent. The second aim was to assess whether and which factors may influence good image quality in order to optimize patient preparation and the diagnostic MR protocol.

Ninety-one MRI scans of the lumbosacral region of dogs without urinary tract disease were retrospectively evaluated by a single operator. Dogs were divided into three groups according

to the patient size and the ureteral path was divided into three segments: proximal, distal, ureterovesical junction. Sixty-four cases met the inclusion criteria.

Ureters appeared on both T1W and T2W sequences as homogeneously hypointense structures visible between the renal pelvis to the urinary bladder. On T2 fat-sat the ureters were never identified. Statistical analysis showed that T2W sequences highlight the ureters with higher quality compared to T1W sequences, and type I chemical shift artefact may be helpful in defining the ureteral contours, especially in the proximal tract. The state of repletion of the colon and urinary bladder also influences the visibility of the ureters mainly along the distal tract and at the level of the ureterovesical junction.

In conclusion, high field MR T2-weighted is feasible to evaluate the ureteral pathway in normal dogs, without the use of contrast medium. However, further studies are needed to assess the

usefulness of T2W sequences for the recognition of pathological conditions of the ureters, such as ureteral ectopia.

Introduction

In veterinary medicine, computed tomography (CT) and ultrasound (US) are the most commonly used imaging modalities for the evaluation of the ureteral tract.

Magnetic resonance (MR) has several limitations for investigating the abdomen and in particular the urinary system. High costs, prolonged anesthesia time and technical issues arising from motion artefacts secondary to cardio-respiratory activity imply that contrast-enhanced CT remains the imaging technique of choice for the evaluation of the upper urinary tract. However, in the last years, with the introduction of respiratory gating and faster protocols, MR has proven to be a valid technique for characterizing upper urinary tract and collecting system disorders in human medicine.

Few studies evaluating MR have been conducted in dogs, and most have focused on vascular perfusion for renal transplantation.[1] In particular, Fonseca-Matheus and colleagues conducted a prospective study describing a MR nephrography protocol which provides adequate time-intensity curve parameters and excellent anatomical detail of the urinary system in dogs, representing an alternative to radionuclide nephrography to assess the renal function.[2] Furthermore, a single case report described a MR protocol for diagnosis of a left retrocaval ureter and transposition of the caudal vena cava in a dog. Authors reported that gadolinium-enhanced MR urography is a superb imaging technique to diagnose retrocaval ureter providing both functional and morphological information.[3]

In human medicine MR is currently considered as a problem-solving imaging technique if CT is non-diagnostic or if CT

cannot be performed, such as in pregnant patients or in cases where contrast medium is contraindicated.

Gadolinium-enhanced MR urography provides both functional information and detailed morphological information on the ureters and periureteral tissue, allowing evaluation of the full spectrum of obstructive and non-obstructive ureteral diseases.[4-5]

Magnetic resonance urography can be performed both with gadolinium-enhanced sequences and with non-enhanced MRI, based on strongly T2-weighted pulse.[4] Static fluid-enhanced MR urography can be employed as an alternative to conventional excretory urography to obtain diagnostic images of the dilated upper urinary tract and adjacent structures. Static fluid-enhanced MR urography does not require the excretion of contrast medium, therefore proved to be useful for evaluating the dilated collector system in a poorly functional kidney, in which the

administration of gadolinium contrast media was contraindicated.[4]

The MRI capability of tracing the anatomy and course of the ureters using T1- and T2-weighted sequences without the use of gadolinium contrast agent has never been investigated in veterinary medicine to the Authors knowledge. This technique could be advantageous in cases where renal excretory function is significantly decreased, and intravenous contrast medium is contraindicated.

The aim of this retrospective design study was to describe the appearance, course and characteristics of the ureters in high-field MR using T1, T2 and T2 weighted fat-saturated sequences. The second aim was to assess whether and which factors may influence good image quality in order to optimize patient preparation and the diagnostic MR protocol.

Material and Method

Experimental design and subject selection criteria

This was a retrospective diagnostic method comparative and descriptive design study.

The medical records of canine patients referred to a single institution (Alphavet Clinic Kifissia, Athens) between December 2021 and August 2022 for MR examination of the lumbosacral spine due to reasons unrelated to disorders of the urinary system were retrospectively reviewed.

Permission to use the clinical and imaging data for research was provided through the informed consent of the owners at the time of admission.

Medical records were reviewed by a third-year PhD student with three years' experience in diagnostic imaging. The following data were recorded: breed, weight, blood analysis. Clinical signs and final diagnosis were not recorded as considered not useful for the purpose of the study.

Dogs were included if the MR examination of the lumbosacral spine with at least T1 and T2 weighted transverse sequences were available, bloodwork including renal parameters (UREA, CREA), urinalysis were unremarkable. Patients were also included if no clinical signs related to the urinary tract were reported. Dogs were excluded if presenting clinical signs related to the urinary tract, if in the MR studies an abdominal suppression band was applied or if the field of view (FOV) was too small to include the entire urinary tract, or if abnormalities were detected on MR examination.

The final decision to include or exclude cases was made on a joint consensus between two ECVDI board-certified radiologists (ML and IP) and a third-year PhD student (CS).

Dogs were divided into three categories according to weight: small (1-10 kg), medium (11-30 kg) and large (>30 kg)- size.

Image acquisition

All dogs were fasted for at least eight hours before the exam. Dogs were sedated with alpha2 agonists (dexmedetomidine), benzodiazepines (midazolam) and opioids (butorphanol, tramadol) at variable combinations and dosages depending on the patient clinical status and weight. Induction was performed with propofol at dosages ranging between 2-3 mg/kg. Maintenance was performed with isofluorane and 100% oxygen with controlled breathing.

A 20- or 22-gauge intravenous catheter was placed in the cephalic vein of all patients, depending on their size. Intravenous fluids were administered throughout the whole MR examination at a maintenance dosage ranging between 5-10 ml/kg/h (Ringer's lactate or NaCl 0.9%).

A 1.5-Tesla whole body MR scanner (General Electric Company GE, United States) was used to perform all the examinations. A large body coil was used for large and medium

breed dogs and a C-spine coil was used for small-size dogs. All dogs were positioned in dorsal recumbency and the standard protocol for evaluation of the spine included: transverse T1WFSE (3D pre- and post-contrast), T2WSE, T2W fat-sat (single shot), T2W STIR, MERGE sequences in transverse or sagittal plane. The post contrast sequence was obtained 10 seconds after intravenous manual injection of 0.1 mmol/kg meglumine gadoterate (Dotarem, Guerbet, France) at a dosage of 0.1 mmol/kg.

Image analyses

The qualitative analysis of the MRI images was performed on a dedicated PACS System (Pureview Image Analyses) by a single operator (CS) under the supervision of an ECVDI board-certified radiologist (ML). The observer was blind to the patient signalment.

The analysis of the images was performed by evaluating

individually each ureter on transverse T1, T2 and T2 fat-sat sequences.

Each ureter was divided into 3 segments: proximal (from the renal pelvis to the aortic bifurcation), distal (from the aortic bifurcation to the vesical trigone) and uretero-vesical junction. The intensity of the ureters was compared to the surrounding fat. The quality and clarity of the ureteral contours was classified according to a 4-point score: 0 not visible, 1 poorly visualized, 2 suboptimal visualization, 3 optimal visualization (Fig.1). The presence of artefacts was recorded. The repletion of the urinary bladder was recorded and subjectively classified as poor, normal, overdistended (Fig. 2). The colon was also described as distended or empty depending on the presence of faecal material and/or gas.

Statistical analysis

Data storage and analysis were performed with IBM SPSS Statistics v. 27.0 (IBM Corp. Armonk. NY). Descriptive

statistics were performed, and categorical variables were expressed as frequencies and percentages.

To evaluate which score allowed to better visualization of the ureters from the renal pelvis to the ureterovesical junction in high-field MR, Chi-square test was performed. Furthermore, the Chi-square test was used to evaluate the influence of dog size, degree of bladder repletion and presence or absence of feces in the colon for the visualization of the ureters. Statistical significance was considered for p value < 0.05.

Results

A total of 91 MRIs of the lumbosacral region were retrospectively evaluated. Twenty-seven cases were excluded because inclusion criteria were not respected. The final sample included a total of 64 MRIs.

Twenty-three dogs were included in the small-size group (36%), 27 in the medium-size group (42%) and 14 in the large-size group (22%).

In twenty-seven dogs the colon was defined empty (42%) while in 37 dogs it contained gas or was distended by fecal content (58%).

The degree of urinary bladder was defined as poor in 12 cases (19%), normal in 39 cases (61%) and overdistended in 13 cases (20%).

The T2W fat-sat sequence was only available in 22/64 studies, and a visibility score of 0 was assigned in all 22 studies in each tract of the right and left ureter, therefore statistical analysis was not performed.

In both T2W and T1W sequences, along the proximal and distal tracts, the ureters appeared homogeneously hypointense in relation to the surrounding hyperintense peritoneal fat. The ureterovesical junction, appeared as a focal thickening of the

urinary bladder wall, at the level of the bladder trigone, iso/hyperintense to the urinary bladder wall on T1 and T2 sequences.

At the level of both proximal ureter on T2 sequences, a type I chemical shift artifact was observed around the ureteral lumen as an hypointense band in 54 cases (84%). At the distal ureter, the same artifact was observed in 35 cases on the left (55%) and in 38 (60%) cases on the right.

At the level of proximal ureters on T1 sequences, a type I chemical shift artifact was observed around the ureteral lumen in 7 cases on the left (11%) and 9 cases on the right (14%). At the distal ureter, the same artefact was observed in 4 cases on the left (6%) and 10 cases on the right (16%).

Ureteral jet was observed bilaterally in two cases (3%).

On T1 sequences the visibility score of the proximal left ureter was assessed as grade 3 in 56/64 cases (86%); the proximal right

ureter was assessed as grade 3 in 57/64 cases (87%). On T2 sequences the visibility score of the proximal left ureter was assessed grade 3 in 55/64 cases (94%); the proximal right ureter was assessed as grade 3 in 60/64 cases (94%).

On T1 sequences the visibility score of the left distal ureter was assessed as grade 3 in 22/64 cases (34%); the right distal ureter was assessed as grade 3 in 30/64 cases (47%).

On T2 sequences the visibility score of the left distal ureter was assessed as grade 3 in 45/64 cases (70%); the right distal ureter was assessed as grade 3 in 51/64 cases (80%).

On T1 sequences the visibility score of the left ureterovesical junction was assessed as grade 3 in 24/66 cases (37%); the right ureterovesical junction was assessed as grade 3 in 24/66 cases (38%). On T2 sequences the visibility score of the left ureterovesical junction was assessed as grade 3 in 35/64 cases (55%); the right ureterovesical junction was assessed as grade 3

in 42/64 cases (66%). The distribution of visibility scores is reported in Table 1.

The statistical analysis performed for each size-category demonstrated that the visibility score of left and right proximal and distal ureter on T2 sequences was significantly higher compared to T1W sequences (proximal right and left p-value <0,001; distal right p-value =0.032; distal left p-value =0.023); The visibility score of both the right and left ureterovesical junction were also significantly higher on the T2 sequences compared to T1 (right and left p-value=0.016).

In the medium-sized dog the visibility score of the left and right proximal ureter on T2 sequences was significantly higher compared to T1 (p-value <0,001). At the level of the right and left distal ureter was not demonstrated a statistically significant difference between T1 and T2 sequences. The right ureteral

junction showed a higher visibility score on T2 sequences compared to T1W (p-value =0.012).

In large-size dog the visibility score of the left and right proximal ureter was assessed as grade 3 in all patients on both T1 and T2 sequences; The visibility score of the left and right distal ureter on T2 sequences was significantly higher compared to T1 (right p-value =0,01; left p-value <0,001); No statistically significant difference between T1 and T2 sequences visibility score distribution was found on the right and left ureterovesical junction.

Distribution of visibility score in each size category is reported in Table 2.

Statistical analysis on urinary bladder appearance showed that both overdistension and poor distension of the urinary bladder are associated with a minor visibility score of the left distal ureter on both T1 and T2 sequences (T1 p-value =0.016; p-

value= 0.011), and of the right and left ureterovesical junctions on T1 and T2 sequences (p-value <0.001).

Statistical analysis on colon repletion grade showed that the presence of faeces and/or gas in the descending colon is associated with a minor visibility score of the ureters in the left distal ureter on both T1 and T2 sequences (T1 p-value =0.009; T2 p-value =0.031) and at left ureterovesical junction on both T1 and T2 sequences (T1 p-value =0.020; T2 p-value =0.015).

Discussion and Conclusion

The results of this study showed that high field MR T1 and T2 sequences allow visualization of the ureters, which appear homogeneously hypointense on both sequences. The T2 sequences tend to highlight the ureters with higher quality compared to T1. The state of repletion of the colon and bladder impacts the visibility of the ureters, mainly along the distal tract and at the ureterovesical junction.

The use of MR for the evaluation of the urinary system was scarcely investigated in veterinary medicine. The main disadvantages of magnetic resonance urography are the elevated cost, limited availability of the system and the low sensitivity in detecting mineralization in case of possible obstructive uropathy. However, the cost of the exam might be justified by the fact that MR provides both excellent anatomical and functional information of the urinary tract. [3]

Recently, a gadolinium-enhanced MR imaging protocol for the evaluation of the urinary tract was described in dogs, in which 3D fat-suppressed echo-gradient sequences were performed before and after contrast-medium administration.[3] Immediately after gadolinium administration an angiographic phase could be obtained, followed by excretory phase after 5 minutes.[3]

The administration of contrast medium may however be contraindicated in patients with renal insufficiency and suspect reduced excretory function of the kidneys, in which gadolinium

contrast medium has been related to nephrogenic systemic fibrosis.[6] Moreover the use of the contrast medium might have an impact in the cost of the exam and might be associated with anaphylaxis.

In human medicine, it is also described that MR urography can provide accurate information about glomerular filtration, similarly to renal scintigraphy. [7-9]

In veterinary medicine, a recent study has shown that MR nephrography is a feasible alternative to scintigraphy nephrography and provides excellent anatomical detail without the application of ionizing radiation. However, the results of this study needed to be validated in animals with normal individual kidney GFR values measured by validated techniques, such as renal scintigraphy. [2]

Magnetic resonance imaging is therefore of potentially great interest for the evaluation of diseases of the urinary system, and

further research is of paramount interest to validate the method and exploit its potential.

The results of the study show that the ureters of healthy dogs are visible on both T1 and T2 sequences as a homogeneously hypointense structure on MR, easily traced between the renal pelvis to the urinary bladder. On T2 sequences, the hyperintense urine fluid signal was never visible within the ureteral lumen. This may be probably due to a lack of administration of diuretic medication before the MR examination, which would have probably increase urine flow rate and output.

Type I chemical shift artefacts are secondary to marked differences in the resonance frequency between water and lipid protons and are created along the edges of abdominal organs.[10-11]

Since the chemical shift effect is directly proportional to the magnetic field strength, they are usually more pronounced at

3.0-T rather than at 1.5- T, and this is reported as a cause of poor images quality in human studies. [12-13]

In our study, type I chemical shift artefact was present in the images obtained on both T1 and T2 sequences, at the proximal and distal ureteral tract. However, it did not affect the assessment of the ureters but instead significantly improved the identification of the ureters. In fact, the artifact resulted in improved definition of the contours of the ureteral lumen and in all sections where chemical shift artefact was observed, a visibility score of 2 or 3 was assigned.

In all patients, motion artefacts never prevented the correct visualization of the ureters. It is likely that controlled breathing and a deep state of anesthesia with a lower respiratory rate played a role in the producing exams of adequate quality.

The results obtained in this study showed that the qualitative assessment of ureters is dependent on the ureteral tract

evaluated, the sequences used, the size of the dog and the state of bladder and colic distension.

The proximal tract of the ureters was clearly visible in small, medium and large dogs, best on T2 sequences. The authors assume that this may be related to the contrast effect of the abundant peritoneal fat in this region and the lack of additional anatomical structures adjacent to the ureters, which may impair their visibility.

At the distal tract level, the ureter was more difficult to follow especially in small-size dogs. Furthermore, the association between a low visibility score and a distended colon and/or an overdistended or poorly distended urinary bladder suggests that an empty colon and a moderately distended urinary bladder may facilitates optimal visualization of the distal ureter, especially on the left ureter. As is logical to assume, in medium and large dogs it was easier to follow the path of the distal tract of the ureters,

although even in these cases the repletion of the colon adversely affected the quality of visibility of the ureters.

The descending colon is commonly distributed in the left caudal abdomen and this might explain while the quality of the exams is particularly affected on the left ureter in case of colonic distention.

The ureterovesical junction was better visualized on T2 sequences in small and medium-sized dogs while in large dogs it was clearly visible on both T1 and T2 sequences. However, in small and medium-sized dogs the visibility score was significantly lower than in large dogs. As above, it is reasonable to assume that the distended colon and/or a poorly distended or overdistended urinary bladder may greatly interfere with proper visualization of the ureterovesical junction in smaller patients.

The ureteral jet was identified in only two dogs out of 64. Indeed, intravenous fluid therapy at a maintenance dosage was administered in all patients. The administration of diuretic drugs

would undoubtedly have increased the likelihood of visualizing the ureteral jet, which is essential to distinguish in case of specific ureteral diseases, such as for intra- or extra-mural ectopic ureters, as previously reported.[14-19]

This study has several limitations, mainly related to the retrospective nature of the work, which led to a lack of a standardized and specific MR protocol for the upper urinary tract. Furthermore, the protocol was not dedicated to visualization of the ureters, but to the evaluation of the lumbosacral tract. However, ureters were visualized in all studies despite the lack of a specific protocol for them.

A higher dosage of fluid therapy or the administration of diuretics could have increased the visibility of the ureteral jet, which was only rarely identified in this study. The length of the exam was also not standardized as the sequences were part of an exam focused in the lumbar area which included the entirety of the urinary tract.

The assessment of the visibility score was performed by only one operator, so it was not possible to calculate the interobserver agreement.

In conclusion, the results of this study demonstrated that high field T2 sequences can be used to evaluate the ureteral pathway in healthy dogs. The proximal tract of the ureters is well visible in both small, medium and large size dogs, whereas for an adequate qualitative evaluation of the distal tract and ureterovesical junction, especially in small-size dogs, it is indicated to perform enema and catheterization of the urinary bladder before the examination, in order to maintain a normal bladder distension and to avoid the colon interfering the visualization of the ureters ate the ureterovesical junctions, particularly on the left side. Further studies are needed to explore the utility of T2 sequences on uro-MR for the evaluation of the

ureters in pathological conditions, such as in case of ureteral ectopia.

	PROXIMAL URETER				DISTAL URETER				URETEROVESCICAL JUNCTION			
	T1		**T2**		**T1**		**T2**		**T1**		**T2**	
	L	R	L	R	L	R	L	R	L	R	L	R
1	2 (3%)	1 (2%)	1 (1%)	0 -	15 (23%)	9 (14%)	7 (11%)	3 (5%)	19 (28%)	17 (26%)	10 (15%)	8 (12%)
2	7 (11%)	8 (11%)	3 (5%)	4 (6%)	27 (42%)	25 (39%)	12 (19%)	10 (15%)	23 (35%)	23 (36%)	19 (30%)	14 (22%)
3	55 (86%)	56 (87%)	55 (94%)	60 (94%)	22 (34%)	30 (47%)	45 (70%)	51 (80%)	24 (37%)	24 (38%)	35 (55%)	42 (66%)

Table 1: Distribution of visibility scores with percentage values of each ureter tract in T1W and T2W sequences calculated on the total sample

		PROXIMAL URETER				DISTAL URETER				UV JUNCTION			
		T1		**T2**		**T1**		**T2**		**T1**		**T2**	
		L	R	L	R	L	R	L	R	L	R	L	R
SMALL-SIZE	**1**	0	0	0	0	6	4	5	2	10	8	5	7
		-	-	-	-	(26%)	(17%)	(22%)	(9%)	(44%)	(34%)	(22%)	(31%)
	2	2	2	0	0	10	6	8	6	11	10	7	5
		(9%)	(9%)	-	-	(43%)	(26%)	(34%)	(26%)	(47%)	(44%)	(31%)	(22%)
	3	21	21	23	23	7	13	10	15	2	5	11	9
		(91%)	(91%)	(100%)	(100%)	(31%)	(57%)	(44%)	(65%)	(9%)	(22%)	(47%)	(47%)
MEDIUM-SIZE	**1**	2	1	0	0	6	3	1	1	10	8	5	2
		(8%)	(4%)	-	-	(23%)	(11%)	(4%)	(4%)	(38%)	(31%)	(19%)	(8%)
	2	5	6	0	0	11	13	2	1	14	10	7	8
		(19%)	(23%)	-	-	(42%)	(56%)	(8%)	(4%)	(54%)	(38%)	(27%)	(31%)
	3	19	19	26	26	9	10	23	24	2	8	14	16
		(73%)	(73%)	(100%)	(100%)	(35%)	(38%)	(88%)	(92%)	(8%)	(31%)	(54%)	(61%)
LARGE-SIZE	**1**	0	0	0	0	3	2	0	0	0	0	1	0
		-	-	-	-	(21%)	(14%)	-	-	-	-	(7%)	-
	2	0	0	0	0	5	5	3	3	7	6	1	1
		-	-	-	-	(36%)	(36%)	(21%)	(21%)	(50%)	(43%)	(7%)	(7%)
	3	14	14	14	14	6	7	11	11	7	8	12	13
		(100%)	(100%)	(100%)	(100%)	(43%)	(50%)	(79%)	(79%)	(50%)	(57%)	(86%)	(93%)

Table 2: Distribution of visibility scores with percentage values of each ureter tract in T1W and T2W sequences calculated for each sample size category

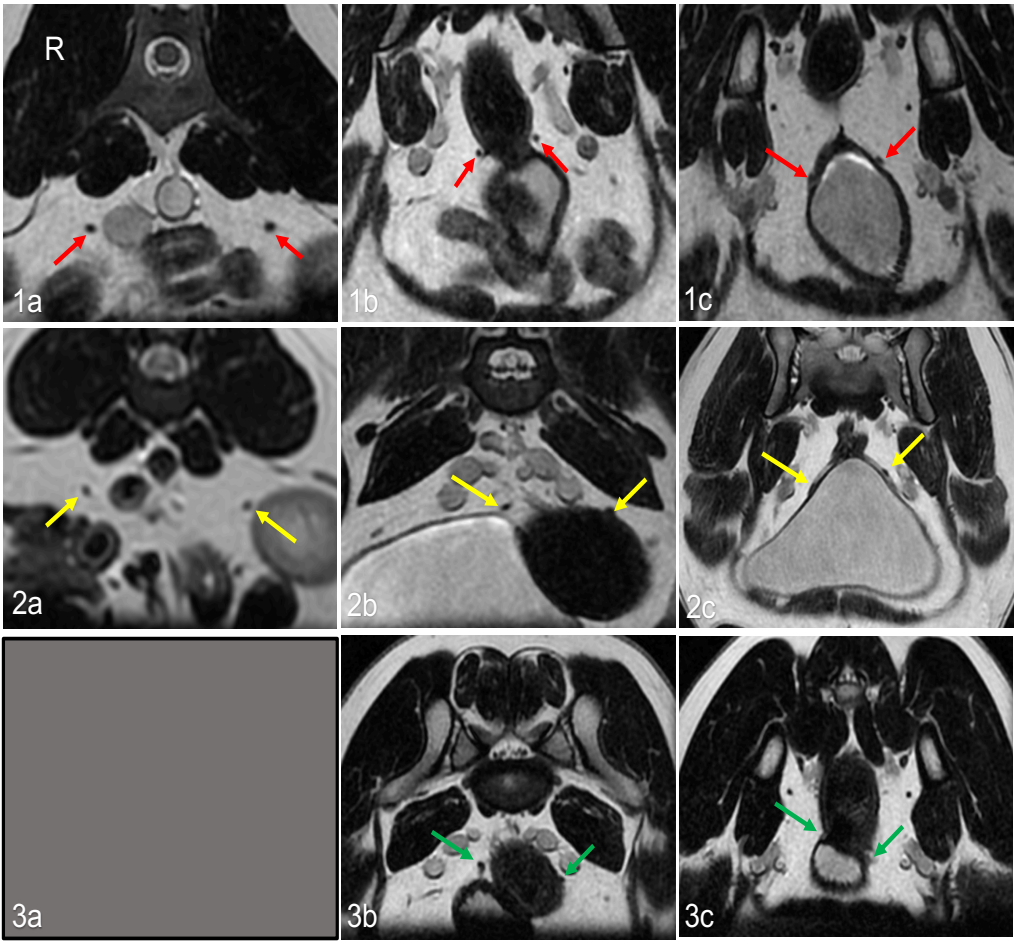

Fig. 1: Cross-sectional images of T2-weighted sequences acquired by high field MR 1.5 T. The images illustrate abdominal tomographic sections at the level of the proximal ureter (1a, 2a), distal ureter (1b, 2b,3b) and ureterovesical junction (1c, 2c, 3c). The red arrows indicate left and right ureters classified as grade 3 of visibility score, the yellow arrows indicate left and right ureters classified as grade 2 of visibility score, green arrows indicate left and right classified as grade 1 of visibility score.

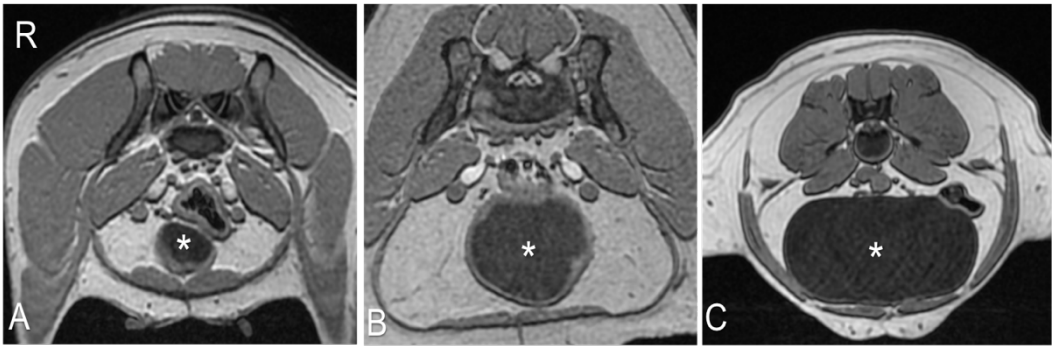

Fig. 2: Cross-sectional images of T1-weighted sequences acquired by high field MR 1.5 T. The images show abdominal tomographic sections at the caudal abdomen. The asterisk indicates the lumen of the urinary bladder defined as poorly distended (A), normally distended (B), or overdistended (C).

Reference

1. Cavrenne R, Mai W. Time-resolved renal contrast-enhanced MRA in normal dogs. Vet Radiol Ultrasound. 2009 Jan-Feb;50(1):58-64. doi: 10.1111/j.1740-8261.2008.01490. x. PMID: 19241755.
2. Fonseca-Matheus JM, Pérez-García CC, Ginja MM, Altónaga JR, Orden MA, Gonzalo-Orden JM. Contrast-enhanced dynamic magnetic resonance nephrography in healthy dogs. Vet J. 2011 Sep;189(3):341-5. doi: 10.1016/j.tvjl.2010.06.025. Epub 2010 Aug 31. PMID: 20810295.
3. Duconseille AC, Louvet A, Lazard P, Valentin S, Molho M. Imaging diagnosis--left retrocaval ureter and transposition of the caudal vena cava in a dog. Vet Radiol Ultrasound. 2010 Jan-Feb;51(1):52-6. doi: 10.1111/j.1740-8261.2009.01621. x. PMID: 20166394.
4. Blandino A, Gaeta M, Minutoli F, et al. MR urography of the ureter. Am J Roentgenol 2002; 179:1307–1314.
5. Leyendecker JR, Barnes CE, Zagoria RJ. MR urography: tech- niques and clinical applications. Radiographics 2008; 28:23–46.
6. Kribben A, Witzke O, Hillen U, Barkhausen J, Daul AE, Erbel R. Nephrogenic systemic fibrosis. Pathogenesis, diagnosis, and therapy. J Am Coll Cardiol 2009; 53:1621–1628.
7. Jones RA, Easley K, Little S, et al. Dynamic contrast-enhanced MR urography in the evaluation of pediatric hydronephrosis: part I, functional assessment. Am J Roentgenol 2005; 185:1598–1607.
8. Jones RA, Perez-Brayfield MR, Kirsch AJ, Grattan-Smith JD. Renal transit time with MR urography in children. Radiology 2004;233: 41–50.
9. Boss A, Martirosian P, Gehrmann M, et al. Quantitative assessment of glomerular filtration rate with MR gadolinium slope clearance measure- ments: a phase I trial. Radiology 2007; 243:783–790.
10. PijlMEJ,DoornbosJ,WasserMNJM,vanHouwelingenHC,Tollenaar RAEM, Bloem JL. Quantitative analysis of focal masses at MR imaging: a plea for standardization. *Radiology*. 2004; 231:737-744.
11. MaiW.*DiagnosticMRIindogsandcats*.1.1. CRCPress;2018;81-102p.
12. BarthMM,SmithMP,PedrosaI,LenkinskiRE,RofskyNM.BodyMR Imaging at 3.0 T: understanding the opportunities and challenges. *Radiographics*. 2007; 27:1445-1462.
13. Kim BR, Ha D-H. Parameters Affecting India Ink Artifacts on Opposed-Phase MR Images. *Investig Magn Reson Imaging*. 2019;23(4): 341-350.
14. Dillman JR, Caoili EM, Cohan RH, Ellis JH, Francis IR, Nan B, Zhang Y. Comparison of urinary tract distension and opacification using single-

bolus 3-Phase vs split-bolus 2-phase multidetector row CT urography. J Comput Assist Tomogr. 2007;31(5):750.
15. Kekelidze M, Dwarkasing RS, Dijkshoorn ML, Sikorska K, Verhagen PC, Krestin GP. Kidney and urinary tract imaging: triple-bolus multidetector CT urography as a one-stop shop-protocol design, opacification, and image quality analysis. Radiology. 2010;255(2):508–16.
16. Dahlman P, Van der Molen AJ, Magnusson M, Magnusson A. How much dose can be saved in three-phase CT urography? A combination of normal- dose corticomedullary phase with low-dose unenhanced and excretory phases. AJR Am J Roentgenol. 2012;199(4):852–60.
17. Mc Nicholas MM, Raptopoulos VD, Schwartz RK, Sheiman RG, Zormpala A, Prassopoulos PK, Ernst RD, Pearlman JD. Excretory phase CT urography for opacification of the urinary collecting system. AJR Am J Roentgenol. 1998; 170(5):1261–7.
18. Roy C, Jeantroux J, Irani FG, Sauer B, et al. Accuracy of intermediate dose of furosemide injection to improve multidetector row CT urography. Eur J Radiol. 2008;66(2):253–61.
19. Secrest S, Essman S, Nagy J, Schultz L. Effects of furosemide on ureteral diameter and attenuation using computed tomographic excretory urography in normal dogs. Vet Radiol Ultrasound. 2013;54(1):17–2

4. DISCUSSION AND CONCLUSION

The urinary tract, including the kidneys, ureters, urinary bladder and urethra, is frequently involved in congenital and acquired diseases. The architecture of these anatomical structures makes them poorly explorable during clinical examination but makes them particularly suitable for investigation by various imaging modalities (Gary Johnston et al).

The development of new methods that allow for a specific investigation of pathology being minimally invasive for the patient is a key point in the diagnosis of urinary tract diseases. At the same time, keeping in mind that only what is known can be recognised, is therefore a must that literature provides a comprehensive collection of possible abnormalities and pathologies that can be found in our patients.

The first work allowed to enrich the existing literature about the use of quantitative CEUS on the urinary tract. In particular we designed a prospective pilot study on a small cohort of canine

patients which allowed to establish useful cut-offs to distinguish neoplastic and non-neoplastic pathologies of the urinary bladder. We concluded that a Fall Time higher than 10.49 s may be the only reliable cut-off to help characterizing neoplastic and non-neoplastic lesions of the urinary bladder in dogs, although this result must be interpreted with caution. A combination of laboratory findings, standard B-mode ultrasound and qualitative and quantitative CEUS analysis is still needed for further evaluation along with cytopathological confirmation.

The second work describes for the first time the presence of a novel CVC congenital malformation in dogs and cats: the transcaval ureter. We concluded that contrast enhanced CT is a suitable method for the diagnosis of transcaval ureter and a focal *double-barrel gun* sign of the CVC is proposed as the hallmark feature of this anomaly. It was not possible to investigate the clinical significance of this alteration due to the small sample size. However, it is certain that it is important to know the

existence of this anomaly in order to prevent any potential medical and surgical complication related to anatomical variation of the CVC, as previously reported both in veterinary and human literature.

In the third and final paper, we described the appearance, course and characteristics of the ureters on T1 and T2 sequences on high field MR without the use of contrast medium. We also focused on factors that could influence image quality. We concluded that the T2 sequences without contrast medium are suitable for assessing the course of the ureters in healthy dogs and that to optimize visualization of the distal ureter and ureterovesical junction it is recommended to perform enema and catheterization of the urinary bladder especially in small and medium-sized dogs.

In this project, we have chosen to focus on anatomical structures and pathologies that represent a daily challenge in clinical routine practice. As previously reported, the ureters are in fact

an anatomical structure that is difficult to investigate using first-level imaging techniques and ureteral pathologies are often associated with subtle and non-specific symptoms. The use of quantitative CEUS to distinguish between neoplastic and non-neoplastic pathologies would instead be an aid during the decision-making phase in which one must choose whether or not to perform biopsy procedures in the case of bladder masses, without incurring the risk of seeding.

The present work not only defines interesting results but also lays the foundations and tips for future research in this field. It will indeed be interesting to assess the clinical significance and possible breed predispositions of transcaval ureter. It will also be interesting to evaluate the appearance of various ureteral pathologies using MR T2 sequences or, eventually, using scanners with different magnetic field powers. In addition, we can explore the applicability of MRI and CEUS for the

assessment of ureterovesical junctions in the course of bladder neoplastic disease, a key step in the formulation of prognosis and therapy.

The main limitation of this project lies in the fact that the data collection is based on spontaneous pathologies and not on induced models, therefore the cohort of patients analyzed is not homogeneous.

In conclusion, the main goal of this project was to produce promising results to reduce the invasiveness of some diagnostic process in case of urinary system diseases. We investigated diagnostic technique that might be more accurate for early diagnosis and, by validating the results, it could reduce the need for invasive procedures such as biopsy to obtain a definitive diagnosis in case of urinary bladder neoplasms. We reported the possibility to avoid the use of paramagnetic contrast medium on MR for evaluation of the ureters, and this is particularly useful

in patients with potential urinary tract disease, whose renal function may already be impaired. Also, we formulated indications for the preparation of the patient in order to optimize the quality of the images for the evaluation of ureters and this could be useful for the purpose of reducing the need to retake scans and reducing anesthesia time. A further goal was to discover a new congenital disease that may have an impact in treatment (ureteral stenting) or could potentially affect renal function itself (CKD). To report congenital anomalies may play an important role in the futures studies on urinary tract disease on small animals.

Received: 24 August 2021 | Revised: 8 March 2022 | Accepted: 10 March 2022

DOI: 10.1111/vru.13105

ORIGINAL INVESTIGATION

WILEY

Fall time may be a reliable discriminator between neoplastic and non-neoplastic urinary bladder lesions in dogs undergoing contrast-enhanced ultrasound: a pilot study

Carlotta Spediacci[1] | Martina Manfredi[1] | Giulia Sala[1] | Tiziana Liuti[2] | Nicolas Israeliantz[2] | Davide Danilo Zani[1] | Mauro Di Giancamillo[1] | Maurizio Longo[1]

[1]Departement of Veterinary Medicine and Animal Science (DIVAS), University of Milan, Street of University n. 6, Lodi (LO) 26900, Italy

[2]Royal Dick School of Veterinary Studies, University of Edinburgh, Edinburgh, Scotland, UK

Corresponding author: Carlotta Spediacci
carlotta.spediacci@unimi.it

Previous Presentation Disclosure: A part of this study was presented at National 74°Conference SISVET 2021 and at VETMEET summer camp 2019.

[Correction added on July 7, 2022, after first online publication: CRUI funding statement has been added.]

Abstract

Contrast-enhanced ultrasound (CEUS) can provide quantitative information on enhancement patterns and perfusion of lesions, based on time-intensity curves (TICs). No published studies have compared CEUS parameters in neoplastic and non-neoplastic urinary bladder lesions in dogs. The aim of the current prospective, pilot study was to quantitatively characterize the CEUS pattern of neoplastic and non-neoplastic urinary bladder lesions in dogs, assessing the influence of contrast arrival time (CAT) on the final appearance of the curves. Fourteen dogs with cyto-histopathological diagnoses were included (seven malignant and seven inflammatory lesions). B-mode ultrasound was performed followed by CEUS examination after an intravenous bolus injection of 0.04 mL/kg of contrast medium, and TICs were elaborated by dedicated software. Receiver operating characteristic curves (ROC) for each TIC parameter were obtained. Neoplastic lesions had subjectively shorter rise time (RT), time to peak (TTP) and fall time (FT) than inflammatory lesions. Based on ROC curve analyses, fall time ≥ 10.49 s was the most reliable parameter for diagnosing non-neoplastic disease in this small sample of dogs (area under the curve [AUC] 0.75, sensitivity 83.33%, specificity 66.67%). No difference was found between ROCs calculated for each parameter of TICs by adding or removing CAT. Results of the current study provide background for future, larger scale studies evaluating use of a CEUS FT threshold of 10.49 s as a possible discriminator for urinary bladder neoplastic lesions in dogs.

KEYWORDS

Canine, Neoplasia, Polypoid cystitis, Bladder Disease, Quantitative CEUS

List of abbreviations: AUC, Area under the curve; CAT, Contrast arrival time; CEUS, Contrast-enhanced ultrasound; CT, Computed Tomography; ECVDI, European College of Veterinary Diagnostic Imaging; FIG, Figure; FT, Fall Time; MHz, Megahertz; mTT, Mean transit time; ROC, Receiver operating Curves; ROI, Region of interest; RT, Rise time; s, Seconds; SI, Maximum signal intensity; SD, Standard deviation; TIC, Time-intensity curve; TTP, Time to peak; UCC, Urothelial cell carcinoma; US, Ultrasound; WHWT, West Highland White Terrier.

frontiers | Frontiers in Veterinary Science

TYPE Original Research
PUBLISHED 08 September 2022
DOI 10.3389/fvets.2022.965185

OPEN ACCESS

EDITED BY
Amalia Agut,
University of Murcia, Spain

REVIEWED BY
Nan Choisunirachon,
Chulalongkorn University, Thailand
Yvonne Espada,
Universitat Autònoma de Barcelona, Spain

*CORRESPONDENCE
Carlotta Spediacci
carlotta.spediacci@unimi.it

SPECIALTY SECTION
This article was submitted to Veterinary Imaging, a section of the journal Frontiers in Veterinary Science

RECEIVED 09 June 2022
ACCEPTED 13 July 2022
PUBLISHED 08 September 2022

CITATION
Spediacci C, Longo M, Specchi S, Pey P, Rabba S, Mavraki E, Di Giancamillo M and Panopoulos I (2022) Computed tomographic appearance of transcaval ureter in two dogs and three cats: A novel CVC congenital malformation. *Front. Vet. Sci.* 9:965185. doi: 10.3389/fvets.2022.965185

Computed tomographic appearance of transcaval ureter in two dogs and three cats: A novel CVC congenital malformation

Carlotta Spediacci[1]*, Maurizio Longo[1,2,3], Swan Specchi[3,4], Pascaline Pey[3,4,5], Silvia Rabba[6], Eirini Mavraki[7], Mauro Di Giancamillo[1] and Ioannis Panopoulos[8]

[1]Department of Veterinary Medicine and Animal Science (DIVAS), University of Milan, Lodi, LO, Italy, [2]Diagnostic Imaging Department C.T.O. Veterinary, via C. Festa Arenzano (Genova), Genova, Italy, [3]Antech Imaging Services, Irvine, CA, United States, [4]Ospedale Veterinario I Portoni Rossi, Bologna, Italy, [5]Service d'Imagerie Médicale, Centre Hospitalier Universitaire Vétérinaire d'Alfort, Ecole Nationale Vétérinaire d'Alfort, Maisons-Alfort, France, [6]Department of Diagnostic Imaging, Istituto Veterinario di Novara, Granozzo con Monticello, NO, Italy, [7]Vets4life Veterinary Clinic, Pikermi, Athens, Greece, [8]Alphavet Veterinary Diagnostic Imaging, Kifisia, Athens, Greece

Transcaval ureter is a rarely reported human congenital malformation of the prerenal segment of the inferior vena cava (IVC) not yet reported in veterinary medicine. The objective of this multicenter retrospective case series study was to describe the computed tomography (CT) features of transcaval ureters in dogs and cats. Patients referring to pre- and post-contrast CT exams of the abdomen and presenting this abnormality were retrospectively included. Multiple qualitative features were described for each ureteral abnormality detected. Three cats and two dogs with transcaval ureter were identified consisting of a segmental duplication of the CVC at the prerenal level creating a vascular ring through which the ureter extended, identified as a *double-barrel gun* sign. The malformation was divided into two types according to the symmetry of the caval branches and location in relation to the aorta, namely, type I symmetrical branches and right-lateral to the aorta, and type II asymmetrically branches and right-dorsal to the aorta. In one case, the malformation was associated with hydroureter and mild pyelectasis. In three cases, the anomaly was incidental and, in the remaining two cases, the clinical significance was uncertain. This is the first study describing the presence of transcaval ureter in dogs and cats. CT was a suitable method for the diagnosis of transcaval and a focal *double-barrel gun* sign of the CVC is proposed as the hallmark feature of this anomaly. The clinical relevance of this congenital vascular malformation is unclear and needs to be further investigated.

KEYWORDS

peri-ureteral venous ring, caudal vena cava malformation, canine, feline, imaging